IEEE Access
Multidisciplinary ⋮ Rapid Review ⋮ Open Access Journal

Received 27 September 2023, accepted 17 October 2023, date of publication 20 October 2023, date of current version 27 October 2023.

Digital Object Identifier 10.1109/ACCESS.2023.3326448

TOPICAL REVIEW

Antiferromagnetic Films and Their Applications

ATSUFUMI HIROHATA[1,2], (Senior Member, IEEE), DAVID C. LLOYD[1], TAKAHIDE KUBOTA[3], (Member, IEEE), TAKESHI SEKI[4], KOKI TAKANASHI[2,4,5], (Senior Member, IEEE), HIROAKI SUKEGAWA[6], (Member, IEEE), ZHENCHAO WEN[6], SEIJI MITANI[6,7], AND HIROKI KOIZUMI[2]

[1]School of Physics, Engineering and Technology, University of York, YO10 5DD York, U.K.
[2]Center for Science and Innovation in Spintronics, Core Research Cluster, Tohoku University, Sendai 980-8579, Japan
[3]Advanced Spintronics Medical Engineering, Graduate School of Engineering, Tohoku University, Sendai 980-0845, Japan
[4]Institute for Materials Research, Tohoku University, Sendai 980-8579, Japan
[5]Advanced Science Research Center, Japan Atomic Energy Agency, Tokai 319-1195, Japan
[6]Research Center for Magnetic and Spintronic Materials, National Institute for Materials Science, Tsukuba 305-0047, Japan
[7]Graduate School of Science and Technology, University of Tsukuba, Tsukuba 305-8577, Japan

Corresponding author: Atsufumi Hirohata (atsufumi.hirohata@york.ac.uk)

This work was supported in part by EU-FP7 Heusler Alloy Replacement for Iridium (HARFIR) under Grant NMP3-SL-2013-604398; in part by the Engineering and Physical Sciences Research Council (EPSRC) under Grant EP/K03278X/1, Grant EP/M02458X/1, and Grant EP/V007211/1; in part by the Japan Science and Technology Agency (JST) Core Research for Evolutional Science and Technology (CREST) under Grant JPMJCR17J5; and in part by the Global Institute for Materials Research Tohoku (GIMRT) of Tohoku University and Ministry of Education, Culture, Sports, Science and Technology (MEXT) Initiative to Establish Next-Generation Novel Integrated Circuits Centers (X-NICS) under Grant JPJ011438.

ABSTRACT Spintronic devices are expected to replace the recent nanoelectronic memories and sensors due to their efficiency in energy consumption and functionality with scalability. To date, spintronic devices, namely magnetoresistive junctions, employ ferromagnetic materials by storing information bits as their magnetization directions. However, in order to achieve further miniaturization with maintaining and/or improving their efficiency and functionality, new materials development is required: 1) increase in spin polarization of a ferromagnet or 2) replacement of a ferromagnet by an antiferromagnet. Antiferromagnetic materials have been used to induce an exchange bias to the neighboring ferromagnet but they have recently been found to demonstrate a 100% spin-polarized electrical current, up to THz oscillation and topological effects. In this review, the recent development of three types of antiferromagnets is summarized with offering their future perspectives towards device applications.

INDEX TERMS Antiferromagnetic materials, Hall effect, magnetoresistance, spintronics, spin polarized transport.

I. INTRODUCTION

Spintronics is one of the emerging fields in condensed matter physics in the view of replacing the recent nanoelectronic devices by improving their efficiency and functionality [1], [2]. In spintronic devices, further improvements are required to continue miniaturization to be comparable with the Si-based semiconductor technology. With a ferromagnet (FM), the miniaturization may induce edge domains and cross-talk between junctions via stray fields, which may prevent fast and reliable operation. On the other hand, using an antiferromagnet (AF), these obstacles can be avoided. Namely for the reduction in power consumption, highly efficient generation and detection of a spin-polarized electrical current need to be developed using the spin-orbit torque, spin caloritronic and topological effects. AF materials and their properties were initially investigated by Néel [3] and have been utilized to exchange couple with the neighboring FM magnetization [4]. This can be measured as a shift in the corresponding magnetization curve as known as an exchange bias (EB) field H_{ex}. H_{ex} has been used to pin one of the FM magnetizations in a FM/non-magnet (NM)/FM trilayer, *i.e.*, a spin-valve structure [5]. This is a basic structure for a read head of a hard disk drive (HDD). By replacing the NM layer with an insulating barrier, a magnetic tunnel junction (MTJ) has been fabricated in a similar manner, which has

The associate editor coordinating the review of this manuscript and approving it for publication was Montserrat Rivas.

been commonly used as the latest HDD read head and a bit cell of a magnetic random access memory (MRAM). For these applications, an $IrMn_3$ alloy has been predominantly employed due to its corrosion resistance and robustness against nanofabrication processes.

Recently, the studies on AF materials and devices have been revitalized after the demonstration of spin polarization by simply flowing an electrical current in an AF layer, which has led to AF spintronics [6], [7], [8]. AF materials have also been demonstrated to generate a spin current at THz frequency [9]. Additionally with the exchange coupling with a FM layer attached, interfacial interactions including Dzyaloshinskii-Moriya interaction (DMI) [10], [11] can be controlled, resulting in the formation of a magnetic skyrmion [12], a semimetal [13] and topological states [14]. These phenomena can offer further improvement in the performance and functionality of spintronic devices.

In parallel, a search for new AF materials which can maintain their AF properties with miniaturisation especially in a film form has been made intensively. There are large variety of AF materials investigated as summarized in Table 1: (i) cubic and (ii) hexagonal structures as shown in Figs. 1 and 2, respectively. The cubic AF includes Group III-VI as appeared in the Periodic Table (*e.g.*, FeO, CoO and NiO [15]), II-VI (*e.g.*, MnO [16], MnS_2, $MnSe_2$ and $MnTe_2$ [16]), Group III (*e.g.*, Cr, FeMn [17] and NiMn [18]) and III-V (*e.g.*, FeN [19] and MnN [20]) compounds as well as ternary/quaternary Heusler alloys (with some atomic substitutions) [21]. The hexagonal AF contains Group III (*e.g.*, $IrMn_3$ [22]), I-III-VI (*e.g.*, $CuFeO_2$ [23], $CuFeS_2$ [24], $CuFeSe_2$ [25] and $CuFeTe_2$ [26]), tetragonal AF (*e.g.*, CuMnAs [27], [28]), antiperovskite manganites [29], [30], [31], [32], [33] and binary Heusler alloys (with some atomic substitutions).

The cubic Heusler alloys crystallize in (i) $L2_1$ phase with X_2YZ composition (full-Heusler) and (ii) $C1_b$ phase with XYZ composition (half-Heusler) [34]. The half-Heusler alloys have an X-vacancy in the unit cell, making them susceptible to atomic displacement. Even for the full-Heusler alloys, the perfectly-ordered $L2_1$ phase can be deformed into the $B2$ phase by atomically displacing Y-Z elements, the $D0_3$ phase by X-Y displacements and the $A2$ phase by randomly exchanging X-Y-Z elements. We have recently found that Ru_2YZ [35], Ni_2YZ [36], [37] and Mn_2YZ [38], [39] Heusler alloys exhibit AF behavior in their $L2_1$, $B2$ and $A2$ crystalline ordering phases. By attaching a FM Fe layer to these AF layers, H_{ex} of up to 600 Oe at 100 K, 90 Oe at 100 K and 30 Oe at 100 K for Ru_2MnGe, Ni_2MnAl and Mn_2Val, respectively, have been found. Mn_2Val is found to maintain its AF properties at room temperature (RT). These differences are found to be induced by the AF alignment of spin moments at the Y site in unique ordered phases. In the ordered $L2_1$ type Ru_2MnZ (Z = Si, Ge, Sn and Sb), the complex AF ordering (2^{nd} type) is a consequence of the frustrated exchange interaction between the Mn atoms. It is concluded that Néel temperature T_N sharply depends on the Z element and that T_N in Ru_2MnGe can be increased by avoiding the disorder in the Mn-Z sub-lattice. For Ni_2MnAl, the (checkerboard-like) AF order only exists in the chemically disordered $B2$ phase due to the large AF nearest neighbor Mn-Mn interaction as schematically shown in Fig. 1. Decreasing the atomic disorder in the Mn-Al sublattice leads to non-zero total magnetization (i.e., ferrimagnet; FI). The excess of Mn or Ni does not improve the anisotropy of the AF state. From the device application point of view, Mn-based AF Heusler alloys are ideal due to their robustness against atomic disordering, especially at the interfaces to neighboring layers.

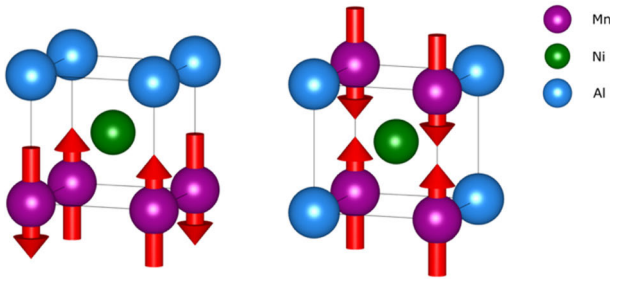

FIGURE 1. Schematic crystalline and spin structures of the pseudo-B2 (I and II) phases for Ni_2MnAl created by VESTA [40].

As Mn-based AF Heusler alloys, binary Heusler alloys with perpendicular anisotropy, such as the $D0_{19}$ Mn_3Z (Z = Ga, Ge and Sn) have been studied to determine their structural and magnetic properties. In perpendicularly anisotropic AF films, the effect of AF-coupled "domains" can be minimized in the in-plane electron scattering as shown schematically in Fig. 2. The Mn_3Ge binary alloy is taken as an example. It allows two stable crystalline structures of the tetragonal $D0_{22}$ and hexagonal $D0_{19}$ structures which is distorted from the basic full-Heusler $L2_1$ structures along the <001> and <111> directions, respectively [41]. As a result of different crystalline structures, the $D0_{22}$ or $D0_{19}$ structure exhibits different magnetic anisotropy such as a FI with perpendicular magnetic anisotropy and low saturation magnetization [42] or AF with noncollinear magnetic moments in which the EB effect [43] appears. Recently, $D0_{19}$ $Mn_{2.8}Ga_{1.2}$ films have been grown with exhibiting H_{ex} up to 430 Oe at 120 K [44], which is almost comparable with recent reports on IrMn with H_{ex} = 688 Oe [45] and MnN (H_{ex} = 3.6 kOe but with less corrosion resistance) [46].

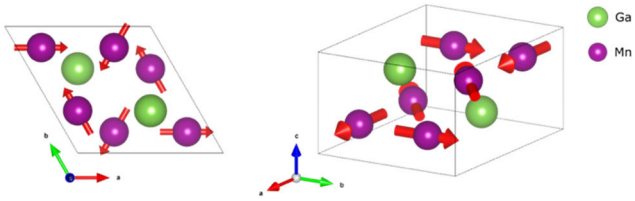

FIGURE 2. Schematic crystalline and spin structures of the $D0_{19}$ phase for Mn_3Ga from the top and side views created by VESTA [40].

TABLE 1. List of major AF materials and their properties. After Refs. [6] and [21]. The bulk and calculate (calc.) values are also included as references.

Group	AF material	Néel temperature [K] (bulk/film/calculation)	Blocking temperature [K] (FM used)	Exchange bias [Oe] (measured temperature)	Magnetic Anisotropy [erg/cm^3]	Ref.
(III)	Cr	311 (bulk)				[21]
	FeMn	333 (bulk)		375 (RT)		[17]
						[47]
	NiMn	797 (bulk)			3.2×10^5	[18]
			>698	650		[48]
				(RT –		[49]
				453 K)		[50]
	PtMn	702 (bulk)		~800 (RT)		[48]
						[51]
	CuMnAs	50 (bulk)				[27]
						[28]
	$IrMn_3$	960 (bulk)				[22]
			463 – 503			[52]
				1.8k (RT)	$\sim 3 \times 10^7$	[53]
	MnF_2	68 (bulk)				[54]
	FeF_2	78 (bulk)				[55]
(II-VI)	MnO	122 (bulk)		~300 (5 K)	2.7×10^4	[15]
						[56]
	MnS	152 (bulk)		290 (5 K)		[16]
						[57]
	MnSe	173 (bulk)				[16]
	MnTe	323 (bulk)	70	~500 (5 K)	$\sim 2.0 \times 10^6$	[16]
			(CrTe)			[58]
	$EuSe_2$	8 ± 0.5 (bulk)				[59]
	EuTe	7.8 ± 0.5 (bulk)		~10 – 142		[52]
				(2 K)		[60]
(III-V)	FeN	100 (bulk)				[19]
	FeP	119 (bulk)				[61]
	FeAs	67 (bulk)				[62]
	FeSb	105 (bulk)				[63]
	MnN	660 (bulk)				[20]
					$\sim 6 \times 10^6$	[53]
	GdP	15				[64]
	GdAs	25				[65]
	GdSb	25				[66]
(III-VI)	FeO	198 (bulk)		~80 (RT)		[15]
						[67]
	CoO	293 (bulk)		1600 (77 K)	5.0×10^6	[4]
			~220 (Co)	400 (170 K)		[15]
						[68]
	NiO	525 (bulk)		133 (RT?)		[15]
						[69]
	Cr_2O_3	310 (bulk)				[70]
				1080		[71]
				(250 K)	$\sim 1.8 \times 10^7$	
						[72]
	$BiFeO_3$	653 (bulk)				[73]
					$\sim 1.0 \times 10^6$	[74]
(Heusler)	Cr_2MnP	240 (calc.)				[75]
	Cr_2MnAs	250 (calc.)				[75]
	Cr_2MnSb	342 (calc.)				[75]
	Cr_2MnBi	320 (calc.)				[75]
	Fe_2VAl					[76]
				16 (100 K)		[77]
	Fe_2VSi	193 (film)				[78]
	Ni_2MnAl	313 (bulk)		>55 (10 K)		[79]
		245 (calc. B2-I)				[80]
		350 (calc. B2-II)				[36]

TABLE 1. *(Continued.)* **List of major AF materials and their properties. After Refs. [6] and [21]. The bulk and calculate (calc.) values are also included as references.**

			≤100 (Fe)			[37]
	$Mn_{2.4}Pt_{0.6}Ga$	120 (bulk)	~90	33k (2 K)		[81]
	Mn_2VAl	>600	~75 (Fe)			[39]
	Mn_2VSi		<100 (CoFe)	34 (100 K)		[38]
	Ru_2MnGe	300 (bulk)				[82]
			126 (Fe)	680 (10 K)		[35]
	Ru_2MnSi	313 (calc.)				[21]
	Ru_2MnSn	296				[21]
	Ru_2MnSb	195				[21]
	Pt_2MnGa	350 (bulk)				[83]
	Mn_3Ge		390			[84]
	Mn_3Ga	470 (bulk)				[85]
		648 (film)	~400	1.5k (RT)	9.1×10^6	[42]
			235	430 (230 K)		[44]
	Mn_3Sn	430 (bulk)				[86]
					2.8×10^3	[87]
	Mn_2FeGa		235 (CoFe, in-plane)	446 (120 K)	-4.8×10^5	[88]
			240 ($[Co/Pt]_3$, perp.)	163 (120 K)		
	$Mn_{2.5}Co_{0.3}Ga_{1.2}$		>350	250 (RT)		[21]
(Antiperovskite)	Mn_3GaN	380 (bulk)				[89]
		345 (film)				[90]
	Mn_3NiN	266 (bulk)				[91]
		250 (film)				[92]
	Mn_3ZnN	183 (bulk)				[91]
	Mn_3AgN	290 (bulk)				[91]
	Mn_3SnN	475 (bulk)				[91]
(Manganite)	$La_{0.45}Sr_{0.55}MnO_3$	220 (film)	~50	98		[29]
						[30]
	$SrMnO_3$	260 (bulk)	~150	$1.0 – 2.0 \times 10^5$		[31]
						[32]
	$CaMnO_3$	122 (bulk)				[33]
(I-II-V)	LiMnSb	>RT(bulk)				[93]
	LiMnAs	374(bulk)				[94]
(I-III-VI)	$CuFeO_2$	11 (bulk)				[23]
	$CuFeS_2$	825 (bulk)				[24]
	$CuFeSe_2$	70 (bulk)				[25]
	$CuFeTe_2$	254 (bulk)				[26]
(II-IV-V)	$MnSiN_2$	490(bulk)				[95]

The major challenge in the development of AF Heusler alloys is that there are over 3000 known Heusler alloy compositions [96]. The key parameter in an AF order is the spacing between planes where the magnetic spins are ordered ferromagnetically in the (001) plane as shown in Figs. 1 and 2 (with slight canting from the plane). Hence it is critical to engineer the composition, so that the right spacing is achieved with typically $B2$ or $D0_{19}$ ordering. This can be confirmed using our recently developed Q-factor analysis as shown in Fig. 3 [37]. The Q-factor is defined as the peak intensity measured by X-ray diffraction (XRD) divided by full width at half maximum, which offers a very simple measure to evaluate the crystallinity of Heusler alloys and beyond.

II. ELECTROMAGNETIC CHARACTERISATIONS

For the characterization of AF materials, the following techniques have been traditionally used: Magnetization measurements with and without a FM layer attached, transport measurements with and without a magnetic field, and synchrotron-based measurements. The former two

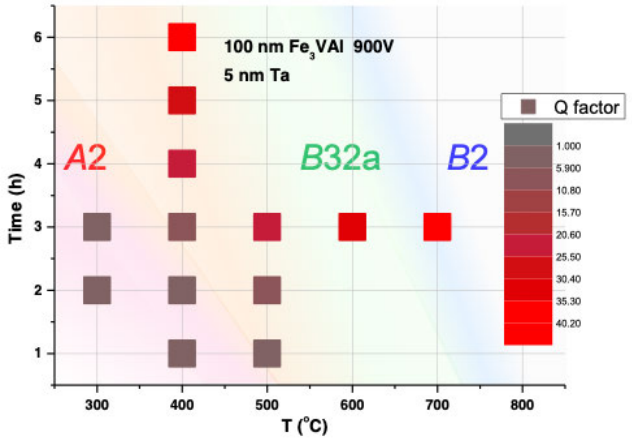

FIGURE 3. Calculated Q-factors and the corresponding crystallization of $Fe_{72.1}V_{14.4}Al_{13.5}$/Ru samples annealed at elevating temperatures.

techniques are relevant for macroscopic analysis, while the last one is sensitive to microscopic characterization as detailed below and Fig. 4.

A. MAGNETIC SUSCEPTIBILITY

In a simplified picture, AF can be treated as two sets of FM-coupled magnetic moments antiparallelly aligned with each other, $M_A = -M_B$ (see Fig. 1). The temperature dependence of this antiparallel alignment can be calculated similar to that of a ferromagnet with the parallel alignment. The antiparallel alignment is stable up to the characteristic temperature, T_N, above which the alignment becomes random due to thermal fluctuation, typically leading to paramagnetic phase [97]. This magnetic phase transition becomes apparent by plotting the temperature dependence of magnetic susceptibility χ. For a single crystal, by applying a magnetic field along the moments, χ increases linearly with increasing temperature T. By applying a field perpendicular to the moments, χ stays constant. For polycrystalline AF, $\chi(T)$ follows between these two cases. Above T_N, χ decreases almost inversely proportional with T, forming a kink in $\chi(T)$ at T_N (see Fig. 4). This method can be useful for a bulk material to generate sufficient change in the magnetic moments, especially in a single phase.

B. EXCHANGE BIAS

As AF does not produce intrinsic magnetization macroscopically, no signal can be detected by a magnetization measurement. Instead, by attaching a FM layer to induce an EB at the interface, a shift of the corresponding FM magnetization curve (H_{ex}) can be measured, the amplitude of which is proportional to the interfacial exchange coupling between AF and FM. This is particularly useful for AF films. H_{ex} can be evaluated by the York Protocol [98]. In an AF/FM bilayer, AF is first set at the setting temperature T_{SET} for 90 min., which is above T_N of AF but below the Curie temperature T_C of the FM film. The bilayer is then cooled to the thermally activated temperature T_{NA}, followed by the heating to the activation temperature T_{ACT} for 30 min. and the magnetization measurement at T_{NA}. In the activation period any activated FM grains reverse their magnetic moments to their originally set direction. This procedure removes the first loop training effect and any thermal activation that may occur during the temperature rise and fall. In polycrystalline bilayers, individual grains have their own blocking temperature T_B, which can be determined by increasing T_{ACT} until the loop shift becomes zero, which represents the median value of T_B ($< T_B >$). $< T_B >$ satisfies the reversed AF volume to be the same with that of the initially set volume [98], which can be an indicative measure of T_N.

C. ELECTRICAL RESISTIVITY AND MAGNETORESISTANCE

Similarly, the temperature dependence of electrical resistivity $\rho(T)$ exhibits a kink in the gradient [21]. Below T_N, antiparallelly-coupled magnetic moments in single-crystal AF can suppress electron scattering. Above T_N, however, the moment alignment becomes random and changes the corresponding resistivity. It should be noted that the changes in the resistivity are found to be 11% maximum, which can be smaller than that due to electron scattering at grain boundaries by over three orders. This is a powerful technique to determine T_N for epitaxial or highly-textured films as well. By applying an external magnetic field during the transport measurements, similar changes in anisotropic magnetoresistance (AMR) [99] and tunneling AMR (TAMR) [100] can be used to determine T_N due to the magnetic phase transformation. TAMR was experimentally demonstrated by Gould et al. with a junction consisting of $Ga_{0.94}Mn_{0.06}As$/Al-O/Ti [101]. A TAMR ratio was found to increase using an AF layer up to 0.15% with a IrMn/MgO/Pt multilayer at room temperature [102]. Recently, AF materials has also been used for TAMR, demonstrating 10% TAMR in IrMn/MgO/Ta junctions [103] and 20% TAMR using CsCl-ordered FeRh magnetic phase transition in FeRh/MgO/FeRh junctions [100].

D. X-RAY MAGNETIC LINEAR DICHROISM

For microscopic evaluation, synchrotron radiation can be used. X-ray magnetic linear dichroism (XMLD) [104] utilizes a pair of linearly polarized soft X-ray with perpendicular polarization. XMLD signals are proportional to the average value of the magnetic moment squared in a domain $<M^2>$. For an AF material, $< M >$ is zero as $M_A = -M_B$ within an AF domain but $<M^2>$ is a finite value, allowing AF domain imaging. Such domain imaging requires a relatively large uniform domain (>a few μm) due to the spatial resolution, which makes it difficult to be used for AF films. Recently, XMLD has been combined with photoemission electron microscopy (PEEM) imaging to achieve sub-μm resolution [105].

E. POLARISED NEUTRON REFLECTIVITY

Another synchrotron-based technique for the characterization of AF materials is polarized neutron reflectivity (PNR). PNR can determine magnetic properties of bulk and layered

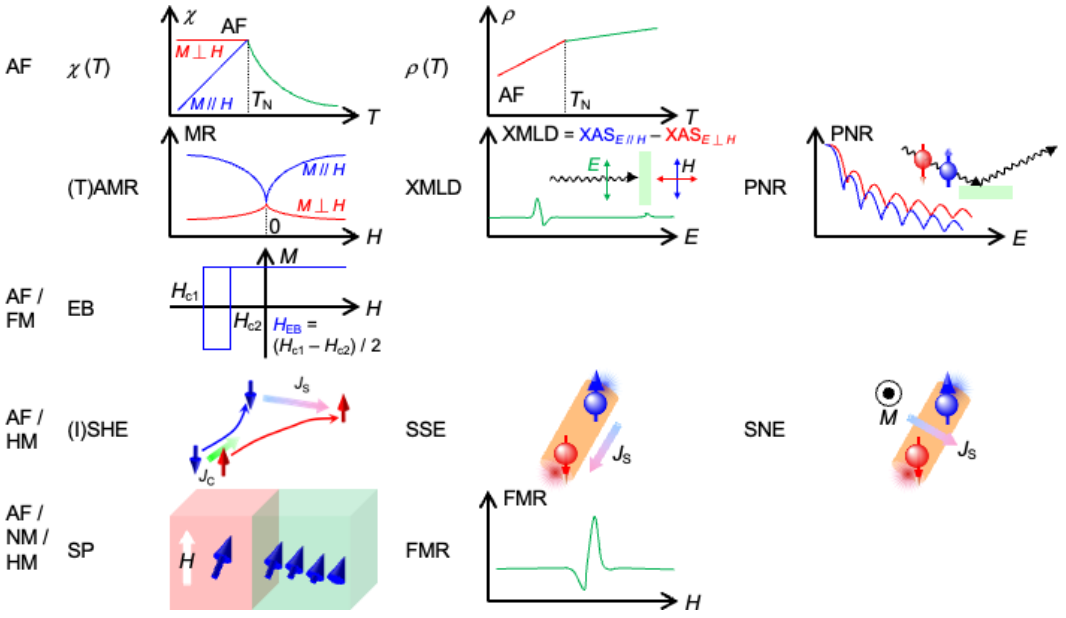

FIGURE 4. List of characterization techniques for AF materials and devices. For AF only, magnetic susceptibility, electrical resistivity and (tunneling) anisotropic magnetoresistance, X-ray magnetic linear dichroism, and polarized neutron reflectivity can be used for characterization as detailed in Sections II-A, C, D and E. By attaching FM and a heavy metal (HM), exchange bias, and (inverse) spin Hall and spin caloritronic effect can indirectly show the AF properties as discussed in Sections II-B and III, respectively. Using a trilayer consisting of AF/NM/HM, spin pumping and ferromagnetic resonance can be used for characterization as described in Section IV.

materials [106]. Due to the magnetic moment of neutron beam interacting with magnetic materials to be imaged, not only layer structures, such as thickness, density, composition and interfacial roughness as similar to X-ray reflectivity (XRR), but also in-plane magnetic moments can be determined. PNR has higher accuracy in a shorter scanning period (<1 min.). The latter magnetic information can be obtained by detecting the neutron reflection with its spins interacted with those in an AF and/or FM layers.

III. SPIN-ORBIT TORQUE

In AF spintronics, three key phenomena can be used for device applications: spin-orbit torque (SOT), spin dynamics and interfacial effects as schematically listed in Fig. 5. These phenomena are discussed in the following sections. In this section, (inverse) spin Hall effects and spin caloritronic effects are reviewed, both of which are induced by SOT.

A. ANOMALOUS HALL AND SPIN HALL EFFECTS

The Hall effect is induced by the Lorentz force under an external magnetic field (ordinary Hall effect). In a magnetic material, anomalous Hall effect (AHE) can be induced due to the spin-orbit interaction, where an effective magnetic field exists by the presence of an intrinsic magnetization. Large AHE was reported in Mn_3Sn [107]. This is due to a weak ferromagnetism induced in the non-colinear AF alignment ($\sim$0.002 μ_B/Mn [87]). Note that additional topological contribution to the Hall signals may need to be considered in a noncolinear magnet [108]. This was employed to develop an AF memory with the writing capability at THz frequency [109].

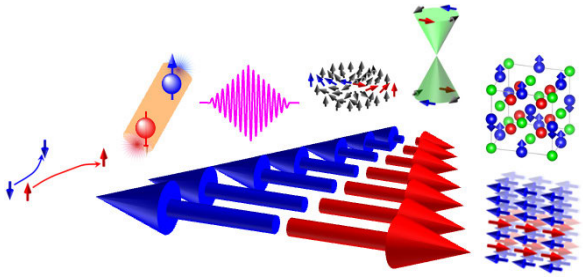

FIGURE 5. Concept of antiferromagnetic spintronics, showing spin Hall effects, spin caloritronics, THz oscillation, magnetic skyrmions, topological effects, Heusler alloys and exchange bias (from left to right).

Spin accumulation in a semiconductor was theoretically predicted by Averikev and Dyakonov under the flow of an electron charge current, introducing the resultant spin current perpendicular to the charge current [110]. This is induced by spin-dependent scattering by an impurity and intrinsic spin-orbit interactions of the material. Averikev and Dyakonov also proposed the inverse effect by aligning the spins by an electromagnetic wave to generate a charge current [111]. These predictions were revisited by Hirsch and named as spin Hall and inverse spin Hall effects (SHE and ISHE), respectively (see Fig. 6) [112]. The relationship between the charge and spin currents can be defined as

$$(\text{Spin current}) = \theta_{SH} \times (\text{Charge current}), \quad (1)$$

where the coefficient θ_{SH} is the spin Hall angle specific to a material used. The corresponding Hamiltonian can be determined as

$$H = \frac{\hbar^2 k^2}{2m} + \lambda_{SO}(\boldsymbol{\sigma} \times \boldsymbol{k}), \tag{2}$$

where $\hbar$: Planck constant divided by 2π, k: wave vector, m: electron mass, λ_{SO}: spin-orbit coupling constant and $\boldsymbol{\sigma}$: spin matrix.

Experimentally, magneto-optical Kerr effect (MOKE) imaging was used to detect the spin accumulation at the edges of GaAs at 30 K, resulting in a spin current of the order of 10 nA/μm^2 [113]. In a similar system, a spin current was also electrically detected [114].

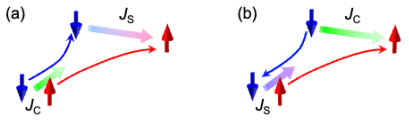

FIGURE 6. Schematic diagram of the (a) SHE and (b) ISHE measurements.

SHE and ISHE do not require an external magnetic field unlike the original Hall effect. When a large magnetic field is applied perpendicular to the material, the accumulated spins start to precess and diminish SHE and ISHE. This induces the corresponding resistance changes with respect to the field, spin Hall magnetoresistance (SHMR) [115]. SHMR was experimentally measured in $Y_3Fe_5O_{12}$ (YIG)/Pt bilayer [116].

In AF materials, large (I)SHE signal has been shown, *e.g.*, (5.3 ± 2.4)% for Mn_3Sn [117], as listed in Table 2. These signals are induced by the spin Hall angles θ_{SH} as listed in Table 2, which are almost one order of magnitude smaller than those for heavy-metals, *e.g.*, −35 (−50)% for W [118] (WOx [119]) and 5.6% for Pt [120].

B. SPIN CALORITRONIC EFFECTS

Spin caloritronic effects, namely spin Seebeck and Nernst effects (SSE and SNE, respectively), can induce a spin current as originally demonstrated in $Ni_{80}Fe_{20}$/Pt [133] and YIG/Pt (see Fig. 7) [134]. In AF materials, a pioneering work was performed with a Cr_2O_3/Pt bilayer by Seki et al. [135] as listed in Table 3. These effects have been intensively investigated for energy harvesting. For SSE, the figure of merit ZT can be determined as [136]

$$ZT\,(\mathrm{SSE}) = \frac{\sigma S^2}{\kappa} T, \tag{3}$$

where T: temperature, σ: electrical conductivity, S: Seebeck coefficient and κ: thermal conductivity. $ZT > 1$ is needed for practical device applications. Similarly for SNE, ZT can be obtained using the Nernst coefficient N as follows:

$$ZT\,(\mathrm{SNE}) = \frac{\sigma N^2}{\kappa} T. \tag{4}$$

An anomalous Nernst effect (ANE) is normally proportional to the intrinsic magnetization of the material under investigation as similar to AHE. Even so, a Nernst signal of ∼0.35 μV/K was reported at RT [135], which is over two orders of magnitude greater than that expected from the weak ferromagnetism [87]. This increase is due to the fact that the transverse thermoelectric conductivity is determined by the Berry curvature in the vicinity of the Fermi level (E_F) offering adiabatic electron motion, while the anomalous Hall conductivity is defined as the sum of the Berry curvature for

TABLE 2. List of spin Hall angle and SMR reported for AF and Weyl materials. After Ref. [7]. SP, SSE and FMR represent spin pumping, spin Seebeck effect and ferromagnetic resonance measurements, respectively.

Group	AF material	Spin diffusion length at RT [nm]	Spin Hall angle θ_{SH} [%]	Ref.
Cubic (III-VI)	NiO	∼3.8		[121]
(III)	Cr		−5.1 ± 0.5 (SP, YIG/Cr)	[122]
			−9 (SSE, YIG/Cr)	
			∼0.7 (Co_2FeAl/Cr)	[123]
				[124]
	FeMn		0.8 ± 0.2 (SP, $Ni_{80}Fe_{20}$/Cu/FeMn)	[125]
			2.2 – 2.8 (FMR, $Ni_{80}Fe_{20}$/Cu/FeMn)	[126]
	PtMn		6 ± 1 (SP, $Ni_{80}Fe_{20}$/Cu/PtMn)	[125]
			6.4 – 8.1 (FMR, $Ni_{80}Fe_{20}$/Cu/PtMn)	[126]
		2.3	24 (SP, $Fe_{50}Co_{30}B_{20}$/Hf/PtMn)	
				[127]
	IrMn		2.2 ± 0.5 (SP, $Ni_{80}Fe_{20}$/Cu/IrMn)	[125]
			5.3 – 9.7 (FMR, $Ni_{80}Fe_{20}$/Cu/IrMn)	[126]
	PdMn		1.5 ± 0.5 (SP, $Ni_{80}Fe_{20}$/Cu/PdMn)	[125]
			2.8 – 4.9 (FMR, $Ni_{80}Fe_{20}$/Cu/PdMn)	[126]
(Heusler)	YPtBi		4.1 (planar Hall, YPtBi/c-Al_2O_3)	[128]
	Co_2MnGa (FM)		−19±4 (planar Hall, Co_2MnGa/MgO(001))	[129]
(III)	$IrMn_3$		∼9, ∼11(111), ∼20(100) (FMR, $Ni_{80}Fe_{20}$/$IrMn_3$)	[130]
	Mn_2Au		0.22 (SP, Mn_3Ga/$Co_{0.2}Fe_{0.6}B_{0.2}$)	[131]
	Mn_3Sn	0.75 ± 0.67	5.3 ± 2.4	[117]
	Mn_3Ga		0.31 ± 0.01 (SP, W/Mn_3Ga/$Co_{0.2}Fe_{0.6}B_{0.2}$)	[132]

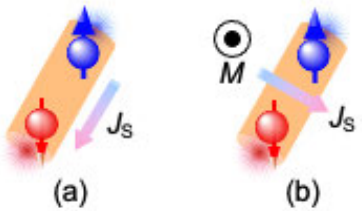

FIGURE 7. Schematic diagram of the (a) SSE and (b) SNE measurements.

TABLE 3. List of spin caloritronic properties reported for AF materials.

Group	AF material	Spin Seebeck coefficient [μV/K]	Spin Nernst coefficient [μV/K]	Figure of merit *ZT*	Ref.
Cubic	NiO	6.5 ± 0.5 (20 K)			[138]
(III-VI)	Cr_2O_3	0.015 (40 K)			[135]
(Heusler)	NiMnSb (FM)	< −2 (100 K)			[139]
	NiTiSn	−155 (300 K)			[140]
	ZrNiSn	~300 (300 K)			[141]
	Co_2TiAl	−55 (300 K)			[140]
	Co_2TiSn	50 (300 K)			[142]
(III)	$IrMn_3$	390 ± 10 (RT)		2.2 (RT)	[143]
Hex.	MnF_2	4.5 (35 K)			[144]
	Mn_3Sn		~0.35 (RT)		[136]

all the occupied bands. Hence, a Weyl metal can be advantageous for spin caloritronic applications due to the unique Berry curvature at Weyl points near E_F [see Fig. 10(b)] The detailed model to calculate the corresponding spin current can be found in Ref. [137].

IV. DYNAMICS

A. SPIN PUMPING

In a FM/AF bilayer, a spin current can be introduced by spin pumping (SP) from FM to AF by precessing the FM magnetization (see Fig. 8). The spin current may be damped in AF and may reduce the reflected spin current into FM, which accordingly increases the damping constant of FM. Using ISHE, the spin current J_S^{SP} satisfies the following relationship [145].

$$V_{ISHE} = wR\theta_{SH}\left(\frac{2e}{\hbar}\right)J_S^{SP}, \tag{5}$$

where w and R are the width and resistance of the bilayered Hall bar and e is the electron charge. V_{ISHE} takes the maximum at the resonant magnetic field, where the maximum precession is achieved and the resulting maximum J_S^{SP} is introduced to AF. Using this condition, θ_{SH} can be estimated as listed in Table 2. This is sensitive to a small spin current to be introduced by increasing R of the Hall bar sample. This technique can also be applied to characterize a spin current generated optically and thermally.

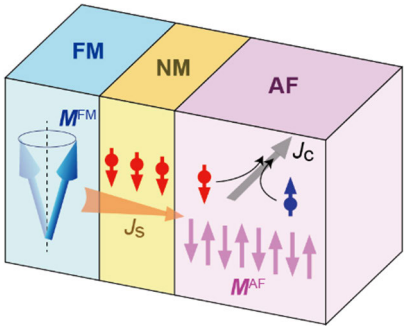

FIGURE 8. Schematic diagram of the spin pumping (SP) measurement in a trilayered structure with ferromagnet (FM)/nonmagnet (NM)/ antiferromagnet (AF). Spin current (J_S) generated by magnetization precession is converted to charge current (J_C) via inverse spin Hall effect in the AF.

B. FERROMAGNETIC RESONANCE

Similar to SP, a FM/AF bilayer is used for ferromagnetic resonance (FMR) as schematically shown in Fig. 9(a). A high-frequency current I (typically at 10 GHz) is applied to a FM/AF bilayer to generate an in-plane radio-frequency (rf) magnetic field perpendicular to the current in the AF layer accompanying with the spin current from the AF layer. This experimental technique is called "spin-torque FMR (ST-FMR)", which was originally employed to evaluate θ_{SH} in the bilayer consisting of FM and NM [146], and has widely been used for a variety of materials [147], [148]. The in-plane rf magnetic field exerts a torque and induces the magnetization precession in the FM layer. At the same time, a spin current can be generated by SHE in the AF and/or at the FM/AF interface, which diffusively flows into the FM layer and exerts a torque perpendicular to the layer. Here, the in-plane torque is in-phase with the high-frequency current, while the perpendicular spin-current torque is shifted by $\pi/2$ from the current frequency. By fitting a FMR spectrum to antisymmetric and symmetric contributions due to the in-plane and perpendicular torques, respectively, ${J_S}^{FMR}$can be estimated from the latter contribution. ${V_{FMR}}^{sym}$ and ${V_{FMR}}^{antisym}$ are given as follows [146] and [149]:

$$V_{FMR}^{sym} = \frac{1}{4}\frac{dR}{d\theta}\frac{\gamma I\cos\theta}{2\pi\left(df/dH\right)_{H=H_0}} \times\left[\frac{\hbar J_S^{FMR}}{2e\mu_0 M_S t_{FM}}\frac{\Delta}{(H-H_0)^2}\right] \tag{6}$$

$$V_{FMR}^{antisym} = \frac{1}{4}\frac{dR}{d\theta}\frac{\gamma I\cos\theta}{2\pi\left(df/dH\right)_{H=H_0}} \times\left[\frac{J_C t_{AF}}{2}\left(1+\frac{e\mu_0 M_S}{\hbar}\right)^{1/2}\frac{(H-H_0)}{\Delta^2+(H-H_0)^2}\right] \tag{7}$$

where $dR/d\theta$: resistance change by the precession, θ: angle between the external magnetic field (H) and I, γ: gyromagnetic constant, f: frequency of I, H_0: FMR field, μ_0: magnetic permittivity in a vacuum ($4\pi \times 10^{-7}$ H/m), M_S: saturation magnetisation of FM, t_{FM}: FM thickness, Δ is half width of half maximum of FMR spectrum, t_{AF}: AF thickness and J_C: charge current.

Using the symmetric and antisymmetric FMR spectrum components, θ_{SH} can be calculated as follows [146]:

$$\theta_{SH} = \frac{J_S^{FMR}}{J_C} = t_{FM} t_{AF} \frac{V_{FMR}^{sym}}{2V_{FMR}^{antisym}} \frac{e\mu_0 M_S}{\hbar} \sqrt{1 + \left(\frac{4\pi M_{eff}}{H}\right)} \tag{8}$$

The literature values of θ_{SH} measured by ST-FMR are listed in Table 2. An example of ST-FMR for the FM/AF bilayer is shown in Fig. 9, in which the $Ni_{81}Fe_{19}$ and $Ir_{22}Mn_{78}$ ($IrMn_{3.55}$) were chosen as FM and AF materials, respectively. Fig. 9(b) displays the optical microscope image of the coplanar-waveguide-shaped device with the sputter deposited $Ni_{81}Fe_{19}$ (3 nm)/$IrMn_{3.55}$ (10 nm) bilayer together with the measurement setup for ST-FMR. The representative ST-FMR spectra are shown in Fig. 9(c), in which the rf current with the frequency of 8 GHz was applied and the in-plane H angles were set at 45° and 225°. The spectra were well fitted with the summation of antisymmetric and symmetric Lorentzian functions. Using Eq. (8), θ_{SH} was evaluated to be 3% for the $IrMn_{3.55}$ alloy.

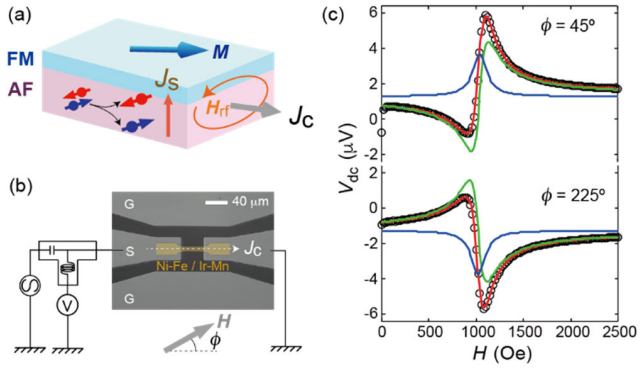

FIGURE 9. (a) Schematic diagram of the spin torque ferromagnetic resonance (ST-FMR) measurement in a bilayer with ferromagnet (FM)/antiferromagnet (AF). (b) optical microscope image of the coplanar-waveguide-shaped device together with the measurement setup. (c) ST-FMR spectra for the $Ni_{81}Fe_{19}$ (3 nm)/$IrMn_{3.55}$ (10 nm) bilayer. The rf current with the frequency of 8 GHz was applied, and the in-plane magnetic field angles were set at 45° and 225°.

C. THz OSCILLATION

By overlaying a direct current (dc) on I in the FMR technique as described in Section IV-B, an effective damping constant of FM M_{eff} can be modified as

$$\Delta\alpha_{eff} = \frac{\sin\theta}{(H + M_{eff}/2)} \frac{\hbar J_S^{FMR}}{2e\mu_0 M_S t_{FM}}. \tag{9}$$

TABLE 4. List of spin dynamics reported for AF materials.

Group	AF material	Gilbert damping constant	Resonant frequency [THz]	Ref.
Cubic (III-VI)	NiO	$(2.1 \pm 0.1) \times 10^{-4}$	1	[152]
	Cr_2O_3		0.240	[152]
	$FeBO_3$		~0.45	[9]
	$TmFeO_3$		~0.8	[9]
	$YFeO_3$		~0.55	[9]
(III)	$IrMn_3$		0.22	[153]

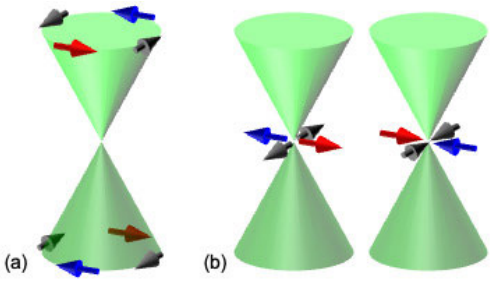

FIGURE 10. Schematic band diagram of the (a) Dirac and (b) Weyl semimetals.

By controlling I, the in-plane and perpendicular torques can be cancelled out, resulting in $\Delta\alpha_{eff} = 0$. This allows oscillation of the FM magnetisation.

THz oscillation can be observed in AF due to strong exchange interactions between two sublattices with M_A and M_B [150], [151]. In NiO, the first demonstration of THz oscillation was achieved [151]. Since then, a great deal of research has been made to achieve higher oscillation frequency in AF materials as listed in Table 4.

V. TOPOLOGICAL EFFECTS AND BEYOND

Topological and interfacial phenomena in AF materials have been intensively investigated recently [154]. For example, Dirac and Weyl semimetals can be formed with AF nature as schematically shown in Fig. 10. The Dirac semimetals form a point connection between the valence and conduction bands at E_F, which is known as the Dirac point. The Dirac point can demonstrate the ideal conductance of $2G_0$ ($G_0 = e^2/h$, where e is the electron charge and h is the Planck constant). The Weyl semimetals contain the chirality at the Dirac point as schematically shown in Fig. 10(b). Weyl semimetals show large AHE, *e.g.*, anomalous Hall angle and conductivity of 0.23 and 60 Ω^{-1}cm^{-1} for GdPtBi [155], 0.11 and 1258.9 for Co_2MnGa, and 0.08 and 1421.6 for Co_2MnAl, respectively [156]. The chiral topological semimetal CoSi shows a small spin Hall angle of $\sim$ 0.03 due to the unique electronic structure [157].

A. MAGNETIC SKYRMIONS

Néel-type magnetic skyrmions were stabilized by attaching $IrMn_3$ underneath $Co_{20}Fe_{60}B_{20}$ at RT [12], which has been supported by theoretical calculations [158]. According to

theoretical prediction, skyrmions in AF can be displaced faster by a smaller critical current density (10^6∼10^7 A/cm^2) than those in conventional FM materials [159], [160]. Although AF skyrmions were stabilized and imaged in a synthetic AF [161] and FI [162], no report has been made to date in AF materials.

B. TOPOLOGICAL EFFECTS

SHE can be induced in an individual layer in two-dimensional $MnBi_2Te_4$, achieving layer Hall effect with up and down spins to be generated at the edges of the top and bottom layers at 1.7 K [163]. This is induced by the layer-locked Berry curvature, which can open a new research field of topological AF spintronics.

C. ORBITAL FERRIMAGNETISM

"Orbital Ferrimagnetism" was firstly termed for FI $CoMnO_3$ by Bozorth et al. [164]. Orbital FI is defined as a system where the net magnetic moment is only attributed to the orbital magnetic momentum. To date, $CoMnO_3$ is the only material known to exhibit orbital FI, consisting of Co^{2+} and Mn^{4+}, which possess $S = 3/2$, respectively. Since these cations are antiferromagnetically coupled, the spin angular momenta cancel each other out. This causes the spin momenta to be compensated, while the orbital angular momentum of Co^{2+} in the crystal field to be conserved. Consequently, the net magnetic moment is proportional to the orbital angular momentum [165], [166]. In other words, an orbital FI has the properties of antiferroic-spin momenta and ferroic-orbital momentum. Therefore, one can expect that the orbital FI would become a bridge between AF spintronics and orbitronics.

D. ALTERMAGNETISM

Recently, a new class of collinear antiferromagnet is theoretically predicted by classifying magnetic material based on spin-group formalism, which is termed as altermagnetism [167], [168]. Altermagnetism is induced by the anisotropic band structure that non-degenerate but equally populated spin-up and spin-down energy isosurfaces. Altermagnetism is predicted to exhibit various spintronics phenomena [169], [170], [171] such as AHE and tunneling magnetoresistance (TMR) similar to AF, and is expected to be a functional material in a novel region of antiferromagnetic spintronics. For example, field-free switching was demonstrated in the heterostructure using RuO_2 [172], [173]. Some other altermagnets, *e.g.*, MnTe [174], [175] and Mn_5Si_3 [176], have also been predicted and characterized.

VI. CONCLUSION AND FUTURE PERSPECTIVES

We have reviewed the recent development and characterization of AF materials and devices. In general, hexagonal (or non-colinear) AF exhibits larger magnetic anisotropy constants of the order of 10 Merg/cm^3, while cubic AF shows smaller constants as summarized in Fig. 11. They correspond to the spin Hall angle θ_{SH} and spin Seebeck/Nernst coefficients. In order to develop efficient AF spintronic devices, higher anisotropy without atomic disordering is needed as highlighted by broad lines. Such materials can be used for an electric-field controlled device [177], SOT-MRAM [178] and energy harvesting [136]. Hall memory concept has also demonstrated with CuMnAs [109] and Mn_2Au [179].

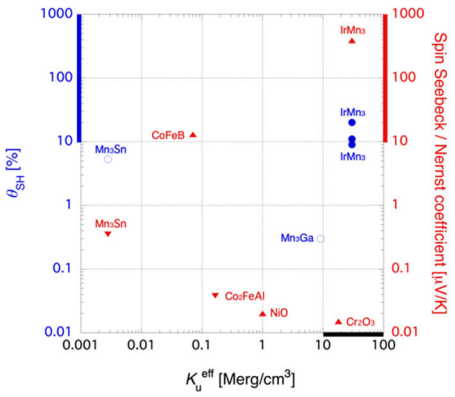

FIGURE 11. Correlations between the magnetic anisotropy constant and the spin Hall angle θ_{SH} (closed symbols) as well as the spin Seebeck/Nernst coefficient (open symbols). After [190], new data added on Mn_3Ga [132] and NiO [137]. Open and closed symbols represent cubic and non-colinear spin configurations, respectively. Blue and red data show θ_{SH} and spin Seebeck and Nernst coefficients, respectively. Target ranges are highlighted as broad lines in the corresponding axes.

TABLE 5. List of abbreviations used in this review.

Abbreviation	Full form
AF	antiferromagnet
AHE	anomalous Hall effect
AMR	Anisotropic magnetoresistance
ANE	anomalous Nernst effect
DMI	Dzyaloshinskii-Moriya interaction
EB	exchange bias
FI	ferrimagnet
FM	ferromagnet
FMR	ferromagnetic resonance
HDD	hard disk drive
HM	heavy metal
ISHE	inverse spin Hall effect
MOKE	magneto-optical Kerr effect
MRAM	magnetic random access memory
MTJ	magnetic tunnel junction
NM	non-magnet
PEEM	photoemission electron microscopy
PNR	polarized neutron reflectivity
RT	room temperature
SHE	spin Hall effect
SHMR	spin Hall magnetoresistance
SNE	spin Nernst effect
SOT	spin-orbit torque
SP	spin pumping
SSE	spin Seebeck effect
ST	spin-torque
Sy	synthetic
TAMR	tunneling anisotropic magnetoresistance
TMR	tunneling magnetoresistance
XAS	X-ray absorption spectroscopy
XMLD	X-ray magnetic linear dichroism
XRD	X-ray diffraction
XRR	X-ray reflectivity

By antiferromagnetically coupling two FM layers through a non-magnetic spacer, a synthetic AF (SyAF) can be formed, which has been commonly used to pin the magnetization of the neighboring FM layer in perpendicularly-magnetized MRAM [180]. Such SyAF has also been used to demonstrate memory operation [181], [182], [183] similar to AF as discussed in Sec. III-A. SyAF can offer broad controllability in the quantization axis in the system, offering design flexibility in AF spintronic devices.

Recently, AF-based magnetic tunnel junctions (MTJs) have been fabricated by showing about a 100% TMR ratio with $Mn_3Pt/MgO/Mn_3Pt$ [184] and 2% ratio with $Mn_3Sn/MgO/Mn_3Sn$ [185]. By enhancing the TMR ratio, such an AF-based MTJ may offer a new architecture for spintronic devices. Such a large TMR ratio is predicted using a noncolinear antiferromagnet, Mn_3Sn [186], and even larger ratio of 500% is predicted with a $RuO_2/TiO_2/RuO_2$ junction [170].

FI can also be used in a similar manner to induce AMR [187], SHE and laser-induced magnetization reversal [188]. The magnetization of FI can be controlled by engineering the composition in the vicinity of the compensation point. This can minimize the corresponding stray field used as an alternative FM in MRAM and magnetic sensors. These AF and FI (as well as a new class of symmetry, altermagnetism [189])-based devices are anticipated to improve the efficiency of their spintronic devices.

REFERENCES

[1] A. Hirohata, K. Yamada, Y. Nakatani, I.-L. Prejbeanu, B. Diény, P. Pirro, and B. Hillebrands, "Review on spintronics: Principles and device applications," *J. Magn. Magn. Mater.*, vol. 509, Sep. 2020, Art. no. 166711, doi: 10.1016/j.jmmm.2020.166711.

[2] B. Dieny et al., "Opportunities and challenges for spintronics in the microelectronics industry," *Nature Electron.*, vol. 3, no. 8, pp. 446–459, Aug. 2020, doi: 10.1038/s41928-020-0461-5.

[3] M. L. Néel, "Propriétés magnétiques des ferrites ferrimagnétisme et antiferromagnétisme," *Annales de Phys.*, vol. 12, no. 3, pp. 137–198, 1948, doi: 10.1051/anphys/194812030137.

[4] W. H. Meiklejohn and C. P. Bean, "New magnetic anisotropy," *Phys. Rev.*, vol. 105, no. 3, pp. 904–913, Feb. 1957, doi: 10.1103/PhysRev.105.904.

[5] R. E. Fontana Jr., B. A. Gurney, T. Lin, V. S. Speriosu, and C. H. Tsang, "Spin valve magnetoresistive sensor with antiparallel pinned layer and improved exchange bias layer, and magnetic recording system using the sensor," U.S. Patent 5 701 223, 1997.

[6] T. Jungwirth, X. Marti, P. Wadley, and J. Wunderlich, "Antiferromagnetic spintronics," *Nature Nanotechnol.*, vol. 11, no. 3, pp. 231–241, Mar. 2016, doi: 10.1038/nnano.2016.18.

[7] V. Baltz, A. Manchon, M. Tsoi, T. Moriyama, T. Ono, and Y. Tserkovnyak, "Antiferromagnetic spintronics," *Rev. Modern Phys.*, vol. 90, no. 1, Feb. 2018, Art. no. 015005, doi: 10.1103/RevModPhys.90.015005.

[8] M. B. Jungfleisch, W. Zhang, and A. Hoffmann, "Perspectives of antiferromagnetic spintronics," *Phys. Lett. A*, vol. 382, no. 13, pp. 865–871, Apr. 2018, doi: 10.1016/j.physleta.2018.01.008.

[9] R. V. Mikhaylovskiy, E. Hendry, A. Secchi, J. H. Mentink, M. Eckstein, A. Wu, R. V. Pisarev, V. V. Kruglyak, M. I. Katsnelson, T. Rasing, and A. V. Kimel, "Ultrafast optical modification of exchange interactions in iron oxides," *Nature Commun.*, vol. 6, no. 1, p. 8190, Sep. 2015, doi: 10.1038/ncomms9190.

[10] I. E. Dzyaloshinskii, "A thermodynamic theory of 'weak' ferromagnetism of antiferromagnetics," *J. Phys. Chem. Solids*, vol. 4, no. 4, pp. 241–255, 1958, doi: 10.1016/0022-3697(58)90076-3.

[11] T. Moriya, "Anisotropic superexchange interaction and weak ferromagnetism," *Phys. Rev.*, vol. 120, no. 1, pp. 91–98, Oct. 1960, doi: 10.1103/PhysRev.120.91.

[12] G. Yu, A. Jenkins, X. Ma, S. A. Razavi, C. He, G. Yin, Q. Shao, Q. L. He, H. Wu, W. Li, W. Jiang, X. Han, X. Li, A. C. Bleszynski Jayich, P. K. Amiri, and K. L. Wang, "Room-temperature skyrmions in an antiferromagnet-based heterostructure," *Nano Lett.*, vol. 18, no. 2, pp. 980–986, Feb. 2018, doi: 10.1021/acs.nanolett.7b04400.

[13] P. Tang, Q. Zhou, G. Xu, and S.-C. Zhang, "Dirac fermions in an antiferromagnetic semimetal," *Nature Phys.*, vol. 12, no. 12, pp. 1100–1104, Aug. 2016, doi: 10.1038/nphys3839.

[14] L. Šmejkal, J. Železný, J. Sinova, and T. Jungwirth, "Electric control of dirac quasiparticles by spin-orbit torque in an antiferromagnet," *Phys. Rev. Lett.*, vol. 118, no. 10, Mar. 2017, Art. no. 106402, doi: 10.1103/PhysRevLett.118.106402.

[15] W. L. Ruth, "Magnetic structures of MnO, FeO, CoO, and NiO," *Phys. Rev.*, vol. 110, no. 6, pp. 1333–1340, Jun. 1958, doi: 10.1103/PhysRev.110.1333.

[16] J. M. Hastings, N. Elliott, and L. M. Corliss, "Antiferromagnetic structures of MnS_2, $MnSe_2$, and $MnTe_2$," *Phys. Rev.*, vol. 115, no. 1, pp. 13–17, Jul. 1959, doi: 10.1103/PhysRev.115.13.

[17] S. Urazhdin and C. L. Chien, "Effects of antiferromagnetic spin rotation on the anisotropy of ferromagnetic/antiferromagnetic bilayers," *Phys. Rev. B, Condens. Matter*, vol. 71, no. 22, Jun. 2005, Art. no. 220410, doi: 10.1103/PhysRevB.71.220410.

[18] J. S. Kasper and J. S. Kouvel, "The antiferromagnetic structure of NiMn," *J. Phys. Chem. Solids*, vol. 11, nos. 3–4, pp. 231–238, Oct. 1959, doi: 10.1016/0022-3697(59)90219-7.

[19] T. Hinomura and S. Nasu, "A study of Fe–N alloy systems," *Hyperfine Interact.*, vol. 111, pp. 221–226, Dec. 1998, doi: 10.1023/A:1012614019538.

[20] A. Leineweber, R. Niewa, H. Jacobs, and W. Kockelmann, "The manganese nitrides η-Mn_3N_2 and θMn_6N_5 + X: Nuclear and magnetic structures," *J. Mater. Chem.*, vol. 10, no. 12, pp. 2827–2834, 2000, doi: 10.1039/B006969H.

[21] A. Hirohata et al., "Development of antiferromagnetic Heusler alloys for the replacement of iridium as a critically raw material," *J. Phys. D, Appl. Phys.*, vol. 50, no. 44, Sep. 2017, Art. no. 443001, doi: 10.1088/1361-6463/aa88f4.

[22] T. Yamaoka, "Antiferromagnetism in γ-phase Mn-Ir alloys," *J. Phys. Soc. Jpn.*, vol. 36, no. 2, pp. 445–450, Feb. 1974, doi: 10.1143/JPSJ.36.445.

[23] K. Hayashi, T. Nozaki, R. Fukatsu, Y. Miyazaki, and T. Kajitani, "Spin dynamics of triangular lattice antiferromagnet $CuFeO_2$: Crossover from spin-liquid to paramagnetic phase," *Phys. Rev. B, Condens. Matter*, vol. 80, no. 14, Oct. 2009, Art. no. 144413, doi: 10.1103/PhysRevB.80.144413.

[24] S. Conejeros, P. Alemany, M. Llunell, I. D. P. R. Moreira, V. Sánchez, and J. Llanos, "Electronic structure and magnetic properties of $CuFeS_2$," *Inorganic Chem.*, vol. 54, no. 10, pp. 4840–4849, May 2015, doi: 10.1021/acs.inorgchem.5b00399.

[25] J. Lamazares, F. Gonzalez-Jimenez, E. Jaimes, L. D'Onofrio, R. Iraldi, G. Sanchez-Porras, M. Quintero, J. Gonzalez, J. C. Woolley and G. Lamarche, "Magnetic, transport, X-ray diffraction and Mössbauer measurements on $CuFeSe_2$," *J. Magn. Magn. Mater.*, vols. 104–107, no. 2, pp. 997–998, Feb. 1992, doi: 10.1016/0304-8853(92)90459-2.

[26] A. Rivas, F. Gonzalez-Jimenez, L. D'Onofrio, E. Jaimes, M. Quintero, and J. Gonzalez, "Mössbauer measurements in $CuFeTe_2$," *Hyperfine Interact.*, vol. 113, pp. 493–498, Aug. 1998, doi: 10.1023/A:1012612808577.

[27] F. Máca, J. Mašek, O. Stelmakhovych, X. Martí, H. Reichlová, K. Uhlířová, P. Beran, P. Wadley, V. Novák, and T. Jungwirth, "Room-temperature antiferromagnetism in CuMnAs," *J. Magn. Magn. Mater.*, vol. 324, no. 8, pp. 1606–1612, Apr. 2012, doi: 10.1016/j.jmmm.2011.12.017.

[28] P. Wadley et al., "Tetragonal phase of epitaxial room-temperature antiferromagnet CuMnAs," *Nature Commun.*, vol. 4, no. 1, p. 2322, Aug. 2013, doi: 10.1038/ncomms3322.

[29] M. Izumi, T. Manako, Y. Konishi, M. Kawasaki, and Y. Tokura, "$La_{1-x}Sr_xMnO_3$ superlattices composed of ferromagnetic x=0.4 and antiferromagnetic x=0.55 layers," *Phys. Rev. B, Condens. Matter*, vol. 61, p. 12187, May 2000, doi: 10.1103/PhysRevB.61.12187.

[30] P. K. Muduli and R. C. Budhani, "Tailoring exchange bias in half-metallic $La_{2/3}Sr_{1/3}MnO_3$ thin films for spin valve applications," *Appl. Phys. Lett.*, vol. 94, no. 20, May 2009, Art. no. 202510, doi: 10.1063/1.3139770.

[31] T. Takeda and S. Ōhara, "Magnetic structure of the cubic perovskite type $SrMnO_3$," *J. Phys. Soc. Jpn.*, vol. 37, no. 1, p. 275, Jul. 1974, doi: 10.1143/JPSJ.37.275.

[32] H. J. Mao, F. Li, L. R. Xiao, Y. Y. Wang, B. Cui, J. J. Peng, F. Pan, and C. Song, "Oscillatory exchange bias effect in $La_{0.67}Sr_{0.33}MnO_3$/G-$SrMnO_3$/$La_{0.67}Sr_{0.33}MnO_3$ sandwiches," *J. Phys. D, Appl. Phys.*, vol. 48, Jun. 2015, Art. no. 295003, doi: 10.1088/0022-3727/48/29/295003.

[33] J. Hejtmánek, Z. Jirák, M. Maryško, C. Martin, A. Maignan, M. Hervieu and B. Raveau, "Interplay between transport, magnetic, and ordering phenomena in $Sm_{1-x}Ca_xMnO_3$," *Phys. Rev. B, Condens. Matter*, vol. 60, p. 14057, Nov. 1999, doi: 10.1103/PhysRevB.60.14057.

[34] A. Hirohata, M. Kikuchi, N. Tezuka, K. Inomata, J. Claydon, Y. Xu, and G. Vanderlaan, "Heusler alloy/semiconductor hybrid structures," *Current Opinion Solid State Mater. Sci.*, vol. 10, no. 2, pp. 93–107, Apr. 2006, doi: 10.1016/j.cossms.2006.11.006.

[35] J. Balluff, T. Huminiuc, M. Meinert, A. Hirohata, and G. Reiss, "Integration of antiferromagnetic Heusler compound Ru_2MnGe into spintronic devices," *Appl. Phys. Lett.*, vol. 111, no. 3, Jul. 2017, Art. no. 032406, doi: 10.1063/1.4985179.

[36] T. Tsuchiya, T. Kubota, T. Sugiyama, T. Huminiuc, A. Hirohata, and K. Takanashi, "Exchange bias effects in Heusler alloy Ni_2MnAl/Fe bilayers," *J. Phys. D, Appl. Phys.*, vol. 49, no. 23, May 2016, Art. no. 235001, doi: 10.1088/0022-3727/49/23/235001.

[37] T. Huminiuc, O. Whear, A. J. Vick, D. C. Lloyd, G. Vallejo-Fernandez, K. O'Grady, and A. Hirohata, "Growth and characterisation of antiferromagnetic Ni_2MnAl Heusler alloy films," *Magnetochemistry*, vol. 7, no. 9, p. 127, Sep. 2021, doi: 10.3390/magnetochemistry7090127.

[38] H. Wu, G. Vallejo-Fernandez, and A. Hirohata, "Magnetic and structural properties of antiferromagnetic Mn_2VSi alloy films grown at elevated temperatures," *J. Phys. D, Appl. Phys.*, vol. 50, no. 37, Aug. 2017, Art. no. 375001, doi: 10.1088/1361-6463/aa80d5.

[39] T. Tsuchiya, R. Kobayashi, T. Kubota, K. Saito, K. Ono, T. Ohhara, A. Nakao, and K. Takanashi, "Mn_2VAl Heusler alloy thin films: Appearance of antiferromagnetism and exchange bias in a layered structure with Fe," *J. Phys. D, Appl. Phys.*, vol. 51, no. 6, Jan. 2018, Art. no. 065001, doi: 10.1088/1361-6463/aaa41a.

[40] K. Momma and F. Izumi, "VESTA 3 for three-dimensional visualization of crystal, volumetric and morphology data," *J. Appl. Crystallogr.*, vol. 44, no. 6, pp. 1272–1276, Dec. 2011, doi: 10.1107/S0021889811038970.

[41] D. Zhang, B. Yan, S.-C. Wu, J. Kübler, G. Kreiner, S. S. P. Parkin, and C. Felser, "First-principles study of the structural stability of cubic, tetragonal and hexagonal phases in Mn_3Z (Z=Ga, Sn and Ge) Heusler compounds," *J. Phys., Condens. Matter*, vol. 25, no. 20, Apr. 2013, Art. no. 206006, doi: 10.1088/0953-8984/25/20/206006.

[42] H. Kurt, N. Baadji, K. Rode, M. Venkatesan, P. Stamenov, S. Sanvito, and J. M. D. Coey, "Magnetic and electronic properties of D22-Mn_3Ge (001) films," *Appl. Phys. Lett.*, vol. 101, no. 13, Sep. 2012, Art. no. 132410, doi: 10.1063/1.4754123.

[43] A. K. Nayak, J. E. Fischer, Y. Sun, B. Yan, J. Karel, A. C. Komarek, C. Shekhar, N. Kumar, W. Schnelle, J. Kübler, C. Felser, and S. S. P. Parkin, "Large anomalous Hall effect driven by a nonvanishing berry curvature in the noncolinear antiferromagnet Mn_3Ge," *Sci. Adv.*, vol. 2, no. 4, Apr. 2016, Art. no. 1501870, doi: 10.1126/sciadv.1501870.

[44] H. Wu, I. Sudoh, R. Xu, W. Si, C. A. F. Vaz, J.-Y. Kim, G. Vallejo-Fernandez, and A. Hirohata, "Large exchange bias induced by polycrystalline Mn_3Ga antiferromagnetic films with controlled layer thickness," *J. Phys. D, Appl. Phys.*, vol. 51, no. 21, May 2018, Art. no. 215003, doi: 10.1088/1361-6463/aabd8e.

[45] K. Elphick, G. Vallejo-Fernandez, T. J. Klemmer, J.-U. Thiele, and K. O'Grady, "HAMR media based on exchange bias," *Appl. Phys. Lett.*, vol. 109, no. 5, Aug. 2016, Art. no. 052402, doi: 10.1063/1.4960300.

[46] P. Zilske, D. Graulich, M. Dunz, and M. Meinert, "Giant perpendicular exchange bias with antiferromagnetic MnN," *Appl. Phys. Lett.*, vol. 110, no. 19, May 2017, Art. no. 192402, doi: 10.1063/1.4983089.

[47] K.-Y. Kim, H.-C. Choi, S.-Y. Jo, and C.-Y. You, "Enhancement of exchange bias field in top-pinned FeMn/Py bilayers with Ta/Cu hybrid underlayers," *J. Appl. Phys.*, vol. 114, no. 7, Aug. 2013, Art. no. 073908, doi: 10.1063/1.4818955.

[48] M. Lederman, "Performance of metallic antiferromagnets for use in spin-valve read sensors," *IEEE Trans. Magn.*, vol. 35, no. 2, pp. 794–799, Mar. 1999, doi: 10.1109/20.750647.

[49] S. Mao, S. Gangopadhyay, N. Amin, and E. Murdock, "NiMn-pinned spin valves with high pinning field made by ion beam sputtering," *Appl. Phys. Lett.*, vol. 69, no. 23, pp. 3593–3595, Dec. 1996, doi: 10.1063/1.117217.

[50] M. Tsunoda, M. Konoto, and M. Takahashi, "Magnetic anisotropy of antiferromagnet in exchange coupled Ni-Fe/Mn-Ni epitaxialbBilayers," *Phys. Stat. Solidi A*, vol. 189, no. 2, p. 449, Feb. 2002, doi: 10.1002/1521-396X.

[51] H. Hoshiya, K. Meguro, and Y. Hamakawa, "Thickness dependence of crystal orientation for annealed MnPt films," *J. Magn. Soc. Jpn.*, vol. 25, nos. 4–2, pp. 831–834, 2001, doi: 10.3379/jmsjmag.25.831.

[52] G. Will, S. J. Pickart, and R. Nathans, "Antiferromagnetic structure of EuTe," *J. Phys. Chem. Solids*, vol. 24, no. 12, pp. 1679–1681, Dec. 1963, doi: 10.1016/0022-3697(63)90116-1.

[53] G. Vallejo-Fernandez and M. Meinert, "Recent developments on MnN for spintronic applications," *Magnetochemistry*, vol. 7, no. 8, p. 116, Aug. 2021, doi: 10.3390/magnetochemistry7080116.

[54] G. P. Felcher and R. Kleb, "Antiferromagnetic domains and the spin-flop transition of MnF_2," *Europhys. Lett.*, vol. 36, no. 6, pp. 455–460, Nov. 1996, doi: 10.1209/epl/i1996-00251-7.

[55] D. P. Belanger, P. Nordblad, A. R. King, V. Jaccarino, L. Lundgren, and O. Beckman, "Critical behavior in anisotropic antiferromagnets," *J. Magn. Magn. Mater.*, vols. 31–34, pp. 1095–1096, Feb. 1983, doi: 10.1016/0304-8853(83)90813-2.

[56] K.-W. Lin, J.-Y. Guo, T.-J. Chen, H. Ouyang, E. Vass, and J. van Lierop, "Correlating exchange bias with magnetic anisotropy in ion-beam bombarded NiFe/Mn-oxide bilayers," *J. Appl. Phys.*, vol. 104, no. 12, Dec. 2008, Art. no. 123908, doi: 10.1063/1.3040719.

[57] X. Chen, A. Hochstrat, P. Borisov, and W. Kleemann, "Successive antiferromagnetic phase transitions in α-MnS probed by the exchange bias effect," *Appl. Phys. Lett.*, vol. 94, no. 3, Jan. 2009, Art. no. 032506, doi: 10.1063/1.3073045.

[58] J. F. Bi, H. Lu, M. G. Sreenivasan, and K. L. Teo, "Exchange bias in zinc-blende CrTe–MnTe bilayer," *Appl. Phys. Lett.*, vol. 94, no. 25, Jun. 2009, Art. no. 252504, doi: 10.1063/1.3157841.

[59] J. A. Cowen, P. Michlin, J. Kraus, S. D. Mahanti, J. A. Aitken, and M. G. Kanatzidis, "$EuSe_2$: A novel antiferromagnetic rare-earth polychalcogenide," *J. Appl. Phys.*, vol. 85, no. 8, pp. 5381–5383, Apr. 1999, doi: 10.1063/1.369984.

[60] W. A. A. Macedo, M. D. Martins, M. J. M. Pires, R. B. Oliveira, C. J. S. M. Pombo, W. C. Nunes, M. Knobel, P. H. O. Rappl, and P. Motisuke, "Exchange bias in Fe/EuTe(111) bilayers," *J. Appl. Phys.*, vol. 102, no. 3, Aug. 2007, Art. no. 033908, doi: 10.1063/1.2767220.

[61] A. S. Sukhanov, S. E. Nikitin, M. S. Pavlovskii, T. C. Sterling, N. D. Andryushin, A. S. Cameron, Y. V. Tymoshenko, H. C. Walker, I. V. Morozov, I. O. Chernyavskii, S. Aswartham, D. Reznik, and D. S. Inosov, "Lattice dynamics in the double-helix antiferromagnet FeP," *Phys. Rev. Res.*, vol. 2, no. 4, Dec. 2020, Art. no. 043405, doi: 10.1103/PhysRevResearch.2.043405.

[62] E. E. Rodriguez, C. Stock, K. L. Krycka, C. F. Majkrzak, P. Zajdel, K. Kirshenbaum, N. P. Butch, S. R. Saha, J. Paglione, and M. A. Green, "Noncollinear spin-density-wave antiferromagnetism in FeAs," *Phys. Rev. B, Condens. Matter*, vol. 83, no. 13, Apr. 2011, Art. no. 134438, doi: 10.1103/PhysRevB.83.134438.

[63] T. Yashiro, Y. Yamaguchi, S. Tomiyoshi, N. Kazama, and H. Watanabe, "Magnetic structure of Fe1+δSb," *J. Phys. Soc. Jpn.*, vol. 34, no. 1, pp. 58–62, Jan. 1973, doi: 10.1143/JPSJ.34.58.

[64] P. Wachter, E. Kaldis, and R. Hauger, "Magnetic exchange interaction in the system GdP-GdS," *Phys. Rev. Lett.*, vol. 40, no. 21, pp. 1404–1407, May 1978, doi: 10.1103/PhysRevLett.40.1404.

[65] E. D. Jones and B. Morosin, "Sign of the nearest-neighbor exchange interaction and its derivative in GdAs," *Phys. Rev.*, vol. 160, no. 2, pp. 451–454, Aug. 1967, doi: 10.1103/PhysRev.160.451.

[66] H. Taub, S. J. Williamson, W. A. Reed, and F. S. L. Hsu, "Specific heat and resistivity of GdSb and HoSb above the Néel temperature," *Solid State Commun.*, vol. 15, no. 2, pp. 185–189, Jul. 1974, doi: 10.1016/0038-1098(74)90737-6.

[67] J. Guo, X. Zhao, Z. Lu, P. Shi, Y. Tian, Y. Chen, S. Yan, L. Bai, and M. Harder, "Evidence for linear dependence of exchange bias on pinned uncompensated spins in an Fe/FeO bilayer," *Phys. Rev. B, Condens. Matter*, vol. 103, no. 5, Feb. 2021, Art. no. 054413, doi: 10.1103/PhysRevB.103.054413.

[68] C.-H.-T. Chang, S.-C. Chang, J.-S. Tsay, and Y.-D. Yao, "Enhanced exchange bias fields for CoO/Co bilayers: Influence of antiferromagnetic grains and mechanisms," *Appl. Surf. Sci.*, vol. 405, pp. 316–320, May 2017, doi: 10.1016/j.apsusc.2017.02.001.

[69] W. Zhu, L. Seve, R. Sears, B. Sinkovic, and S. S. P. Parkin, "Field cooling induced changes in the antiferromagnetic structure of NiO films," *Phys. Rev. Lett.*, vol. 86, no. 23, pp. 5389–5392, Jun. 2001, doi: 10.1103/PhysRevLett.86.5389.

[70] B. N. Brockhouse, "Antiferromagnetic structure in Cr_2O_3," *J. Chem. Phys.*, vol. 21, no. 5, pp. 961–962, May 1953, doi: 10.1063/1.1699098.

[71] Y. Shiratsuchi, Y. Tao, K. Toyoki, and R. Nakatani, "Magnetoelectric induced switching of perpendicular exchange bias using 30-nm-thick Cr_2O_3 thin film," *Magnetochemistry*, vol. 7, no. 3, p. 36, Mar. 2021, doi: 10.3390/magnetochemistry7030036.

[72] I. Banerjee, H. K. D. Kim, D. Pisani, K. P. Mohanchandra, and G. P. Carman, "Magnetic anisotropy and magnetodielectric coefficients in Cr_2O_3 and $Fe_{0.4}Cr_{1.6}O_3$," *J. Alloys Compounds*, vol. 614, pp. 305–309, Nov. 2014, doi: 10.1016/j.jallcom.2014.06.038.

[73] T. Zhao, A. Scholl, F. Zavaliche, K. Lee, M. Barry, A. Doran, M. P. Cruz, Y. H. Chu, C. Ederer, N. A. Spaldin, R. R. Das, D. M. Kim, S. H. Baek, C. B. Eom, and R. Ramesh, "Electrical control of antiferromagnetic domains in multiferroic $BiFeO_3$ films at room temperature," *Nature Mater.*, vol. 5, no. 10, pp. 823–829, Sep. 2006, doi: 10.1038/nmat1731.

[74] V. S. Rusakov, V. S. Pokatilov, A. S. Sigov, M. E. Matsnev, and A. P. Pyatakov, "Analysis of the magnetic structure of the $BiFeO_3$ multiferroic by Mössbauer spectroscopy," *Doklady Phys.*, vol. 63, no. 6, pp. 223–226, Jul. 2018, doi: 10.1134/S1028335818060113.

[75] I. Galanakis, K. Özdoğan, E. Şaşioğlu, and B. Aktaş, "Ab initiodesign of half-metallic fully compensated ferrimagnets: The case of Cr_2MnZ (Z=P, As, Sb, and Bi)," *Phys. Rev. B, Condens. Matter*, vol. 75, no. 17, May 2007, Art. no. 172405, doi: 10.1103/PhysRevB.75.172405.

[76] D. J. Singh and I. I. Mazin, "Electronic structure, local moments, and transport in Fe_2VAl," *Phys. Rev. B, Condens. Matter*, vol. 57, no. 22, pp. 14352–14356, Jun. 1998, doi: 10.1103/PhysRevB.57.14352.

[77] T. Huminiuc, O. Whear, T. Takahashi, J.-Y. Kim, A. Vick, G. Vallejo-Fernandez, K. O'Grady, and A. Hirohata, "Growth and characterisation of ferromagnetic and antiferromagnetic $Fe_{2+x}V_yAl$ Heusler alloy films," *J. Phys. D, Appl. Phys.*, vol. 51, no. 32, Jul. 2018, Art. no. 325003, doi: 10.1088/1361-6463/aacf4c.

[78] N. Fukatani, K. Ueda, and H. Asano, "Epitaxial strain and antiferromagnetism in Heusler Fe_2VSi thin films," *J. Appl. Phys.*, vol. 109, no. 7, Apr. 2011, Art. no. 073911, doi: 10.1063/1.3555089.

[79] M. Acet, E. Duman, E. F. Wassermann, L. Mañosa, and A. Planes, "Coexisting ferro- and antiferromagnetism in Ni_2MnAl Heusler alloys," *J. Appl. Phys.*, vol. 92, no. 7, pp. 3867–3871, Sep. 2002, doi: 10.1063/1.1504498.

[80] I. Galanakis and E. Şaşioğlu, "Structural-induced antiferromagnetism in Mn-based full Heusler alloys: The case of Ni_2MnAl," *Appl. Phys. Lett.*, vol. 98, no. 10, Mar. 2011, Art. no. 102514, doi: 10.1063/1.3565246.

[81] A. K. Nayak, M. Nicklas, S. Chadov, P. Khuntia, C. Shekhar, A. Kalache, M. Baenitz, Y. Skourski, V. K. Guduru, A. Puri, U. Zeitler, J. M. D. Coey, and C. Felser, "Design of compensated ferrimagnetic Heusler alloys for giant tunable exchange bias," *Nature Mater.*, vol. 14, no. 7, pp. 679–684, Mar. 2015, doi: 10.1038/nmat4248.

[82] S. Mizusaki, T. Ohnishi, A. Douzono, M. Hirose, Y. Nagata, M. Itou, Y. Sakurai, T. C. Ozawa, H. Samata, and Y. Noro, "The role of 3D electrons in the appearance of ferromagnetism in the antiferromagnetic Ru_2MnGe Heusler compound: A magnetic Compton scattering study," *J. Phys., Condens. Matter*, vol. 24, no. 25, May 2012, Art. no. 255601, doi: 10.1088/0953-8984/24/25/255601.

[83] S. Singh, S. W. D'Souza, J. Nayak, E. Suard, L. Chapon, A. Senyshyn, V. Petricek, Y. Skourski, M. Nicklas, C. Felser, and S. Chadov, "Room-temperature tetragonal non-collinear Heusler antiferromagnet Pt_2MnGa," *Nature Commun.*, vol. 7, no. 1, p. 12671, Aug. 2016, doi: 10.1038/ncomms12671.

[84] J. F. Qian, A. K. Nayak, G. Kreiner, W. Schnelle, and C. Felser, "Exchange bias up to room temperature in antiferromagnetic hexagonal Mn_3Ge," *J. Phys. D, Appl. Phys.*, vol. 47, no. 30, Jul. 2014, Art. no. 305001, doi: 10.1088/0022-3727/47/30/305001.

[85] E. Krén and G. Kádár, "Neutron diffraction study of Mn_3Ga," *Solid State Commun.*, vol. 8, no. 20, pp. 1653–1655, Oct. 1970, doi: 10.1016/0038-1098(70)90484-9.

[86] T. F. Duan, W. J. Ren, W. L. Liu, S. J. Li, W. Liu, and Z. D. Zhang, "Magnetic anisotropy of single-crystalline Mn_3Sn in triangular and helix-phase states," *Appl. Phys. Lett.*, vol. 107, no. 8, Aug. 2015, Art. no. 082403, doi: 10.1063/1.4929447.

[87] S. Tomiyoshi and Y. Yamaguchi, "Magnetic structure and weak ferromagnetism of Mn_3Sn studied by polarized neutron diffraction," *J. Phys. Soc. Jpn.*, vol. 51, no. 8, pp. 2478–2486, Aug. 1982, doi: 10.1143/JPSJ.51.2478.

[88] T. Ogasawara, E. Jackson, M. Tsunoda, Y. Ando, and A. Hirohata, "In-plane and perpendicular exchange bias effect induced by an antiferromagnetic $D0_{19}$ Mn_2FeGa thin film," *J. Magn. Magn. Mater.*, vol. 484, pp. 307–312, Aug. 2019, doi: 10.1016/j.jmmm.2019.04.024.

[89] W. J. Feng, D. Li, Y. F. Deng, Q. Zhang, H. H. Zhang, and Z. D. Zhang, "Magnetic and transport properties of $Mn_{3+x}Ga_{1-x}N$ compounds," *J. Mater. Sci.*, vol. 45, no. 10, pp. 2770–2774, Feb. 2010, doi: 10.1007/s10853-010-4265-2.

[90] T. Nan et al., "Controlling spin current polarization through non-collinear antiferromagnetism," *Nature Commun.*, vol. 11, no. 1, p. 4671, Sep. 2020, doi: 10.1038/s41467-020-17999-4.

[91] D. Fruchart and E. F. Bertaut, "Magnetic studies of the metallic perovskite-type compounds of manganese," *J. Phys. Soc. Jpn.*, vol. 44, no. 3, pp. 781–791, Mar. 1978, doi: 10.1143/JPSJ.44.781.

[92] D. Boldrin, I. Samathrakis, J. Zemen, A. Mihai, B. Zou, F. Johnson, B. D. Esser, D. W. McComb, P. K. Petrov, H. Zhang, and L. F. Cohen, "Anomalous Hall effect in noncollinear antiferromagnetic Mn_3NiN thin films," *Phys. Rev. Mater.*, vol. 3, no. 9, Sep. 2019, Art. no. 094409, doi: 10.1103/PhysRevMaterials.3.094409.

[93] G. Achenbach and H. Schuster, "Ternäre verbindungen des lithiums und natriums mit Mangan und elementen der 5. Hauptgruppe," *Zeitschrift für Anorganische und Allgemeine Chem.*, vol. 475, no. 4, pp. 9–17, Apr. 1981, doi: 10.1002/zaac.19814750403.

[94] W. Bronger, P. Mueller, R. Hoeppner, and H. U. Schuster, "The magnetic properties of NaMnP, NaMnAs, NaMnSb, NaMnBi, LiMnAs and KMnAs, characterized by neutron-diffraction experiments," *Z. Anorg. Allg. Chem.*, vol. 539, no. 1, pp. 175–182, Jan. 1986, doi: 10.1002/CHIN.198701022.

[95] H. Watanabe and Y. Yanase, "Symmetry analysis of current-induced switching of antiferromagnets," *Phys. Rev. B, Condens. Matter*, vol. 98, no. 22, Dec. 2018, Art. no. 220412, doi: 10.1103/PhysRevB.98.220412.

[96] K. Elphick, W. Frost, M. Samiepour, T. Kubota, K. Takanashi, H. Sukegawa, S. Mitani, and A. Hirohata, "Heusler alloys for spintronic devices: Review on recent development and future perspectives," *Sci. Technol. Adv. Mater.*, vol. 22, no. 1, pp. 235–271, Dec. 2021, doi: 10.1080/14686996.2020.1812364.

[97] S. Chikazumi, *Physics of Ferromagnetism*. Oxford, U.K.: Oxford Univ. Press, 1997, pp. 134–159.

[98] K. O'Grady, L. E. Fernandez-Outon, and G. Vallejo-Fernandez, "A new paradigm for exchange bias in polycrystalline thin films," *J. Magn. Magn. Mater.*, vol. 322, no. 8, pp. 883–899, Apr. 2010, doi: 10.1016/j.jmmm.2009.12.011.

[99] I. Fina, X. Marti, D. Yi, J. Liu, J. H. Chu, C. Rayan-Serrao, S. Suresha, A. B. Shick, J. Železný, T. Jungwirth, J. Fontcuberta, and R. Ramesh, "Anisotropic magnetoresistance in an antiferromagnetic semiconductor," *Nature Commun.*, vol. 5, no. 1, p. 4671, Sep. 2014, doi: 10.1038/ncomms5671.

[100] X. Z. Chen, J. F. Feng, Z. C. Wang, J. Zhang, X. Y. Zhong, C. Song, L. Jin, B. Zhang, F. Li, M. Jiang, Y. Z. Tan, X. J. Zhou, G. Y. Shi, X. F. Zhou, X. D. Han, S. C. Mao, Y. H. Chen, X. F. Han, and F. Pan, "Tunneling anisotropic magnetoresistance driven by magnetic phase transition," *Nature Commun.*, vol. 8, no. 1, p. 449, Sep. 2017, doi: 10.1038/s41467-017-00290-4.

[101] C. Gould, C. Rüster, T. Jungwirth, E. Girgis, G. M. Schott, R. Giraud, K. Brunner, G. Schmidt, and L. W. Molenkamp, "Tunneling anisotropic magnetoresistance: A spin-valve-like tunnel magnetoresistance using a single magnetic layer," *Phys. Rev. Lett.*, vol. 93, no. 11, Sep. 2004, Art. no. 117203, doi: 10.1103/PhysRevLett.93.117203.

[102] B. G. Park, J. Wunderlich, D. A. Williams, S. J. Joo, K. Y. Jung, K. H. Shin, K. Olejník, A. B. Shick, and T. Jungwirth, "Tunneling anisotropic magnetoresistance in multilayer-(Co/Pt)/AlO_x/PtStructures," *Phys. Rev. Lett.*, vol. 100, no. 8, Feb. 2008, Art. no. 087204, doi: 10.1103/PhysRevLett.100.087204.

[103] D. Petti, E. Albisetti, H. Reichlová, J. Gazquez, M. Varela, M. Molina-Ruiz, A. F. Lopeandía, K. Olejník, V. Novák, I. Fina, B. Dkhil, J. Hayakawa, X. Marti, J. Wunderlich, T. Jungwirth, and R. Bertacco, "Storing magnetic information in IrMn/MgO/Ta tunnel junctions via field-cooling," *Appl. Phys. Lett.*, vol. 102, no. 19, May 2013, Art. no. 192404, doi: 10.1063/1.4804429.

[104] G. van der Laan, N. D. Telling, A. Potenza, S. S. Dhesi, and E. Arenholz, "Anisotropic X-ray magnetic linear dichroism and spectromicroscopy of interfacial Co/NiO(001)," *Phys. Rev. B, Condens. Matter*, vol. 83, no. 6, Feb. 2011, Art. no. 064409, doi: 10.1103/PhysRevB.83.064409.

[105] K. Arai, T. Okuda, A. Tanaka, M. Kotsugi, K. Fukumoto, T. Ohkochi, T. Nakamura, T. Matsushita, T. Muro, M. Oura, Y. Senba, H. Ohashi, A. Kakizaki, C. Mitsumata, and T. Kinoshita, "Three-dimensional spin orientation in antiferromagnetic domain walls of NiO studied by X-ray magnetic linear dichroism photoemission electron microscopy," *Phys. Rev. B, Condens. Matter*, vol. 85, no. 10, Mar. 2012, Art. no. 104418, doi: 10.1103/PhysRevB.85.104418.

[106] J. A. C. Bland, "Polarized neutron reflection," in *Ultrathin Magnetic Structures I*, J. A. C. Bland and B. Heinrich, Eds. Berlin, Germany: Springer, 1994, pp. 305–343.

[107] S. Nakatsuji, N. Kiyohara, and T. Higo, "Large anomalous Hall effect in a non-collinear antiferromagnet at room temperature," *Nature*, vol. 527, no. 7577, pp. 212–215, Oct. 2015, doi: 10.1038/nature15723.

[108] N. Kanazawa, Y. Onose, T. Arima, D. Okuyama, K. Ohoyama, S. Wakimoto, K. Kakurai, S. Ishiwata, and Y. Tokura, "Large topological Hall effect in a short-period helimagnet MnGe," *Phys. Rev. Lett.*, vol. 106, no. 15, Apr. 2011, Art. no. 156603, doi: 10.1103/PhysRevLett.106.156603.

[109] K. Olejník, T. Seifert, Z. Kašpar, V. Novák, P. Wadley, R. P. Campion, M. Baumgartner, P. Gambardella, P. Němec, J. Wunderlich, J. Sinova, P. Kužel, M. Müller, T. Kampfrath, and T. Jungwirth, "Terahertz electrical writing speed in an antiferromagnetic memory," *Sci. Adv.*, vol. 4, no. 3, Mar. 2018, Art. no. eaar3566, doi: 10.1126/sciadv.aar3566.

[110] M. I. Dyakonov and V. I. Perel, "Possibility of orientating electron spins with current," *Sov. Phys. JETP Lett.*, vol. 13, no. 11, pp. 467–469, Jun. 1971. [Online]. Available: http://jetpletters.ru/ps/1587/article_24366.shtml

[111] M. I. Dyakonov and V. I. Perel, "Current-induced spin orientation of electrons in semiconductors," *Phys. Lett. A*, vol. 35, no. 6, pp. 459–460, Jul. 1971, doi: 10.1016/0375-9601(71)90196-4.

[112] J. E. Hirsch, "Spin Hall effect," *Phys. Rev. Lett.*, vol. 83, no. 9, pp. 1834–1837, Aug. 1999, doi: 10.1103/PhysRevLett.83.1834.

[113] Y. K. Kato, R. C. Myers, A. C. Gossard, and D. D. Awschalom, "Observation of the spin Hall effect in semiconductors," *Science*, vol. 306, no. 5703, pp. 1910–1913, Dec. 2004, doi: 10.1126/science.1105514.

[114] J. Wunderlich, B. Kaestner, J. Sinova, and T. Jungwirth, "Experimental observation of the spin-Hall effect in a two-dimensional spin-orbit coupled semiconductor system," *Phys. Rev. Lett.*, vol. 94, no. 4, Feb. 2005, Art. no. 047204, doi: 10.1103/PhysRevLett.94.047204.

[115] M. I. Dyakonov, "Magnetoresistance due to edge spin accumulation," *Phys. Rev. Lett.*, vol. 99, no. 12, Sep. 2007, Art. no. 126601, doi: 10.1103/PhysRevLett.99.126601.

[116] H. Nakayama, M. Althammer, Y.-T. Chen, K. Uchida, Y. Kajiwara, D. Kikuchi, T. Ohtani, S. Geprägs, M. Opel, S. Takahashi, R. Gross, G. E. W. Bauer, S. T. B. Goennenwein, and E. Saitoh, "Spin Hall magnetoresistance induced by a nonequilibrium proximity effect," *Phys. Rev. Lett.*, vol. 110, no. 20, May 2013, Art. no. 206601, doi: 10.1103/PhysRevLett.110.206601.

[117] P. K. Muduli, T. Higo, T. Nishikawa, D. Qu, H. Isshiki, K. Kondou, D. Nishio-Hamane, S. Nakatsuji, and Y. Otani, "Evaluation of spin diffusion length and spin Hall angle of the antiferromagnetic Weyl semimetal Mn_3Sn," *Phys. Rev. B, Condens. Matter*, vol. 99, no. 18, May 2019, Art. no. 184425, doi: 10.1103/PhysRevB.99.184425.

[118] C.-F. Pai, L. Liu, Y. Li, H. W. Tseng, D. C. Ralph, and R. A. Buhrman, "Spin transfer torque devices utilizing the giant spin Hall effect of tungsten," *Appl. Phys. Lett.*, vol. 101, no. 12, Sep. 2012, Art. no. 122404, doi: 10.1063/1.4753947.

[119] K.-U. Demasius, T. Phung, W. Zhang, B. P. Hughes, S.-H. Yang, A. Kellock, W. Han, A. Pushp, and S. S. P. Parkin, "Enhanced spin–orbit torques by oxygen incorporation in tungsten films," *Nature Commun.*, vol. 7, no. 1, p. 10644, Feb. 2016, doi: 10.1038/ncomms10644.

[120] J.-C. Rojas-Sánchez, N. Reyren, P. Laczkowski, W. Savero, J.-P. Attané, C. Deranlot, M. Jamet, J.-M. George, L. Vila, and H. Jaffrès, "Spin pumping and inverse spin Hall effect in platinum: The essential role of spin-memory loss at metallic interfaces," *Phys. Rev. Lett.*, vol. 112, no. 10, Mar. 2014, Art. no. 106602, doi: 10.1103/PhysRevLett.112.106602.

[121] Y. Chen, E. Cogulu, D. Roy, J. Ding, J. B. Mohammadi, P. G. Kotula, N. A. Missert, M. Wu, and A. D. Kent, "Spin transport in an insulating ferrimagnetic-antiferromagnetic-ferrimagnetic trilayer as a function of temperature," *AIP Adv.*, vol. 9, no. 10, Oct. 2019, Art. no. 105319, doi: 10.1063/1.5116549.

[122] C. Du, H. Wang, F. Yang, and P. C. Hammel, "Systematic variation of spin-orbit coupling with D-orbital filling: Large inverse spin Hall effect in 3D transition metals," *Phys. Rev. B, Condens. Matter*, vol. 90, no. 14, Oct. 2014, Art. no. 140407, doi: 10.1103/PhysRevB.90.140407.

[123] D. Qu, S. Y. Huang, and C. L. Chien, "Inverse spin Hall effect in Cr: Independence of antiferromagnetic ordering," *Phys. Rev. B, Condens. Matter*, vol. 92, no. 2, Jul. 2015, Art. no. 020418, doi: 10.1103/PhysRevB.92.020418.

[124] Z. Wen, J. Kim, H. Sukegawa, M. Hayashi, and S. Mitani, "Spin-orbit torque in Cr/CoFeAl/MgO and Ru/CoFeAl/MgO epitaxial magnetic heterostructures," *AIP Adv.*, vol. 6, no. 5, Mar. 2016, Art. no. 056307, doi: 10.1063/1.4944339.

[125] W. Zhang, M. B. Jungfleisch, W. Jiang, J. E. Pearson, A. Hoffmann, F. Freimuth, and Y. Mokrousov, "Spin Hall effects in metallic antiferromagnets," *Phys. Rev. Lett.*, vol. 113, no. 19, Nov. 2014, Art. no. 196602, doi: 10.1103/PhysRevLett.113.196602.

[126] W. Zhang, M. B. Jungfleisch, F. Freimuth, W. Jiang, J. Sklenar, J. E. Pearson, J. B. Ketterson, Y. Mokrousov, and A. Hoffmann, "All-electrical manipulation of magnetization dynamics in a ferromagnet by antiferromagnets with anisotropic spin Hall effects," *Phys. Rev. B, Condens. Matter*, vol. 92, no. 14, Oct. 2015, Art. no. 144405, doi: 10.1103/PhysRevB.92.144405.

[127] Y. Ou, S. Shi, D. C. Ralph, and R. A. Buhrman, "Strong spin Hall effect in the antiferromagnet PtMn," *Phys. Rev. B, Condens. Matter*, vol. 93, no. 22, Jun. 2016, Art. no. 220405, doi: 10.1103/PhysRevB.93.220405.

[128] T. Shirokura, T. Fan, N. H. D. Khang, T. Kondo, and P. N. Hai, "Efficient spin current source using a half-Heusler alloy topological semimetal with back end of line compatibility," *Sci. Rep.*, vol. 12, no. 1, p. 2426, Feb. 2022, doi: 10.1038/s41598-022-06325-1.

[129] L. Leiva, S. Granville, Y. Zhang, S. Dushenko, E. Shigematsu, T. Shinjo, R. Ohshima, Y. Ando, and M. Shiraishi, "Giant spin Hall angle in the Heusler alloy Weyl ferromagnet Co_2MnGa," *Phys. Rev. B, Condens. Matter*, vol. 103, no. 4, Jan. 2021, doi: 10.1103/PhysRevB.103.L041114.

[130] W. Zhang, W. Han, S.-H. Yang, Y. Sun, Y. Zhang, B. Yan and S. S. P. Parkin, "Giant facet-dependent spin-orbit torque and spin Hall conductivity in the triangular antiferromagnet $IrMn_3$," *Sci. Adv.*, vol. 2, no. 2, Sep. 2016, Art. no. e1600759, doi: 10.1126/sciadv.1600759.

[131] B. B. Singh and S. Bedanta, "Large spin Hall angle and spin-mixing conductance in the highly resistive antiferromagnet Mn_2Au," *Phys. Rev. Appl.*, vol. 13, no. 4, Apr. 2020, Art. no. 044020, doi: 10.1103/PhysRevApplied.13.044020.

[132] B. B. Singh, K. Roy, J. A. Chelvane, and S. Bedanta, "Inverse spin Hall effect and spin pumping in the polycrystalline noncollinear antiferromagnetic Mn_3Ga," *Phys. Rev. B, Condens. Matter*, vol. 102, no. 17, Nov. 2020, Art. no. 174444, doi: 10.1103/PhysRevB.102.174444.

[133] K. Uchida, S. Takahashi, K. Harii, J. Ieda, W. Koshibae, K. Ando, S. Maekawa, and E. Saitoh, "Observation of the spin Seebeck effect," *Nature*, vol. 455, no. 7214, pp. 778–781, Oct. 2008, doi: 10.1038/nature07321.

[134] S. Meyer, Y.-T. Chen, S. Wimmer, M. Althammer, T. Wimmer, R. Schlitz, S. Geprägs, H. Huebl, D. Ködderitzsch, H. Ebert, G. E. W. Bauer, R. Gross, and S. T. B. Goennenwein, "Observation of the spin Nernst effect," *Nature Mater.*, vol. 16, no. 10, pp. 977–981, Sep. 2017, doi: 10.1038/nmat4964.

[135] S. Seki, T. Ideue, M. Kubota, Y. Kozuka, R. Takagi, M. Nakamura, Y. Kaneko, M. Kawasaki, and Y. Tokura, "Thermal generation of spin current in an antiferromagnet," *Phys. Rev. Lett.*, vol. 115, no. 26, Dec. 2015, Art. no. 266601, doi: 10.1103/PhysRevLett.115.266601.

[136] M. Mizuguchi and S. Nakatsuji, "Energy-harvesting materials based on the anomalous Nernst effect," *Sci. Technol. Adv. Mater.*, vol. 20, no. 1, pp. 262–275, Mar. 2019, doi: 10.1080/14686996.2019.1585143.

[137] Y. Takezoe, K. Hosono, A. Takeuchi, and G. Tatara, "Theory of spin transport induced by a temperature gradient," *Phys. Rev. B, Condens. Matter*, vol. 82, no. 9, Sep. 2010, Art. no. 094451, doi: 10.1103/PhysRevB.82.094451.

[138] A. Prakash, J. Brangham, F. Yang, and J. P. Heremans, "Spin Seebeck effect through antiferromagnetic NiO," *Phys. Rev. B, Condens. Matter*, vol. 94, no. 1, Jul. 2016, Art. no. 014427, doi: 10.1103/PhysRevB.94.014427.

[139] S. Gardelis, J. Androulakis, P. Migiakis, J. Giapintzakis, S. K. Clowes, Y. Bugoslavsky, W. R. Branford, Y. Miyoshi, and L. F. Cohen, "Synthesis and physical properties of arc melted NiMnSb," *J. Appl. Phys.*, vol. 95, no. 12, pp. 8063–8068, Jun. 2004, doi: 10.1063/1.1739293.

[140] S. Ouardi, G. H. Fecher, B. Balke, X. Kozina, G. Stryganyuk, C. Felser, S. Lowitzer, D. Ködderitzsch, H. Ebert and E. Ikenaga, "Electronic transport properties of electron- and hole-doped semiconducting $C1_b$ Heusler compounds: $NiTi_{1-x}M_xSn$ ($M = Sc, V$)," *Phys. Rev. B, Condens. Matter*, vol. 82, Art. no. 085108, 2010, doi: 10.1103/PhysRevB.82.085108.

[141] H. Muta, T. Kanemitsu, K. Kurosaki, and S. Yamanaka, "High-temperature thermoelectric properties of nb-doped MNiSn (M=Ti, Zr) half-Heusler compound," *J. Alloys Compounds*, vol. 469, nos. 1–2, pp. 50–55, Feb. 2009, doi: 10.1016/j.jallcom.2008.02.041.

[142] S. Chatterjee, S. Chatterjee, S. Giri, and S. Majumdar, "Transport properties of Heusler compounds and alloys," *J. Phys., Condens. Matter*, vol. 34, no. 1, Jan. 2022, Art. no. 013001, doi: 10.1088/1361-648X/ac268c.

[143] S. Tu et al., "Record thermopower found in an IrMn-based spintronic stack," *Nature Commun.*, vol. 11, no. 1, p. 2023, Apr. 2020, doi: 10.1038/s41467-020-15797-6.

[144] M. Kimata, H. Chen, K. Kondou, S. Sugimoto, P. K. Muduli, M. Ikhlas, Y. Omori, T. Tomita, A. H. MacDonald, S. Nakatsuji, and Y. Otani, "Magnetic and magnetic inverse spin Hall effects in a non-collinear antiferromagnet," *Nature*, vol. 565, no. 7741, pp. 627–630, Jan. 2019, doi: 10.1038/s41586-018-0853-0.

[145] A. Ruiz-Calaforra, T. Brächer, V. Lauer, P. Pirro, B. Heinz, M. Geilen, A. V. Chumak, A. Conca, B. Leven, and B. Hillebrands, "The role of the non-magnetic material in spin pumping and magnetization dynamics in NiFe and CoFeB multilayer systems," *J. Appl. Phys.*, vol. 117, no. 16, Apr. 2015, Art. no. 163901, doi: 10.1063/1.4918909.

[146] L. Liu, T. Moriyama, D. C. Ralph, and R. A. Buhrman, "Spin-torque ferromagnetic resonance induced by the spin Hall effect," *Phys. Rev. Lett.*, vol. 106, no. 3, Jan. 2011, Art. no. 036601, doi: 10.1103/PhysRevLett.106.036601.

[147] T. Seki, S. Iihama, T. Taniguchi, and K. Takanashi, "Large spin anomalous Hall effect in $L1_0$-FePt: Symmetry and magnetization switching," *Phys. Rev. B, Condens. Matter*, vol. 100, no. 14, Oct. 2019, Art. no. 144427, doi: 10.1103/PhysRevB.100.144427.

[148] T. Seki, Y.-C. Lau, S. Iihama, and K. Takanashi, "Spin-orbit torque in a Ni-Fe single layer," *Phys. Rev. B, Condens. Matter*, vol. 104, no. 9, Sep. 2021, Art. no. 094430, doi: 10.1103/PhysRevB.104.094430.

[149] A. Layadi and J. O. Artman, "Study of antiferromagnetic coupling by ferromagnetic resonance (FMR)," *J. Magn. Magn. Mater.*, vol. 176, nos. 2–3, pp. 175–182, Dec. 1997, doi: 10.1016/S0304-8853(97)00142-X.

[150] T. Satoh, S.-J. Cho, R. Iida, T. Shimura, K. Kuroda, H. Ueda, Y. Ueda, B. A. Ivanov, F. Nori, and M. Fiebig, "Spin oscillations in antiferromagnetic NiO triggered by circularly polarized light," *Phys. Rev. Lett.*, vol. 105, no. 7, Aug. 2010, Art. no. 077402, doi: 10.1103/PhysRevLett.105.077402.

[151] T. Kampfrath, A. Sell, G. Klatt, A. Pashkin, S. Mährlein, T. Dekorsy, M. Wolf, M. Fiebig, A. Leitenstorfer, and R. Huber, "Coherent terahertz control of antiferromagnetic spin waves," *Nature Photon.*, vol. 5, no. 1, pp. 31–34, Jan. 2011, doi: 10.1038/nphoton.2010.259.

[152] J. Li, C. B. Wilson, R. Cheng, M. Lohmann, M. Kavand, W. Yuan, M. Aldosary, N. Agladze, P. Wei, M. S. Sherwin, and J. Shi, "Spin current from sub-terahertz-generated antiferromagnetic magnons," *Nature*, vol. 578, no. 7793, pp. 70–74, Jan. 2020, doi: 10.1038/s41586-020-1950-4.

[153] M. Chen, R. Mishra, Y. Wu, K. Lee, and H. Yang, "Terahertz emission from compensated magnetic heterostructures," *Adv. Opt. Mater.*, vol. 6, no. 17, Jun. 2018, Art. no. 1800430, doi: 10.1002/adom.201800430.

[154] L. Šmejkal, Y. Mokrousov, B. Yan, and A. H. MacDonald, "Topological antiferromagnetic spintronics," *Nature Phys.*, vol. 14, no. 3, pp. 242–251, Mar. 2018, doi: 10.1038/s41567-018-0064-5.

[155] C. Shekhar, N. Kumar, V. Grinenko, S. Singh, R. Sarkar, H. Luetkens, S.-C. Wu, Y. Zhang, A. C. Komarek, E. Kampert, Y. Skourski, J. Wosnitza, W. Schnelle, A. McCollam, U. Zeitler, J. Kübler, B. Yan, H.-H. Klauss, S. S. P. Parkin, and C. Felser, "Anomalous Hall effect in Weyl semimetal half-Heusler compounds RPtBi (R = Gd and Nd)," *Proc. Nat. Acad. Sci. USA*, vol. 115, no. 37, pp. 9140–9144, Sep. 2018, doi: 10.1073/pnas.1810842115.

[156] Y. Ji, W. Zhang, H. Zhang, and W. Zhang, "Spin Hall conductivity and anomalous Hall conductivity in full Heusler compounds," *New J. Phys.*, vol. 24, no. 5, May 2022, Art. no. 053027, doi: 10.1088/1367-2630/ac696c.

[157] K. Tang, Y.-C. Lau, K. Nawa, Z. Wen, Q. Xiang, H. Sukegawa, T. Seki, Y. Miura, K. Takanashi, and S. Mitani, "Spin Hall effect in a spin-1 chiral semimetal," *Phys. Rev. Res.*, vol. 3, no. 3, Jul. 2021, Art. no. 033101, doi: 10.1103/PhysRevResearch.3.033101.

[158] S. von Malottki, B. Dupé, P. F. Bessarab, A. Delin, and S. Heinze, "Enhanced skyrmion stability due to exchange frustration," *Sci. Rep.*, vol. 7, no. 1, p. 12299, Sep. 2017, doi: 10.1038/s41598-017-12525-x.

[159] J. Barker and O. A. Tretiakov, "Static and dynamical properties of antiferromagnetic skyrmions in the presence of applied current and temperature," *Phys. Rev. Lett.*, vol. 116, no. 14, Apr. 2016, Art. no. 147203, doi: 10.1103/PhysRevLett.116.147203.

[160] X. Zhang, Y. Zhou, and M. Ezawa, "Antiferromagnetic skyrmion: Stability, creation and manipulation," *Sci. Rep.*, vol. 6, no. 1, p. 24795, Apr. 2016, doi: 10.1038/srep24795.

[161] W. Legrand, D. Maccariello, F. Ajejas, S. Collin, A. Vecchiola, K. Bouzehouane, N. Reyren, V. Cros, and A. Fert, "Room-temperature stabilization of antiferromagnetic skyrmions in synthetic antiferromagnets," *Nature Mater.*, vol. 19, no. 1, pp. 34–42, Jan. 2020, doi: 10.1038/s41563-019-0468-3.

[162] S. Woo, K. M. Song, X. Zhang, Y. Zhou, M. Ezawa, X. Liu, S. Finizio, J. Raabe, N. J. Lee, S.-I. Kim, S.-Y. Park, Y. Kim, J.-Y. Kim, D. Lee, O. Lee, J. W. Choi, B.-C. Min, H. C. Koo, and J. Chang, "Current-driven dynamics and inhibition of the skyrmion Hall effect of ferrimagnetic skyrmions in GdFeCo films," *Nature Commun.*, vol. 9, no. 1, p. 959, Mar. 2018, doi: 10.1038/s41467-018-03378-7.

[163] A. Gao et al., "Layer Hall effect in a 2D topological axion antiferromagnet," *Nature*, vol. 595, no. 7868, pp. 521–525, Jul. 2021, doi: 10.1038/s41586-021-03679-w.

[164] R. M. Bozorth and D. E. Walsh, "Ferromagnetic moment of $CoMnO_3$," *J. Phys. Chem. Solids*, vol. 5, no. 4, pp. 299–301, Jan. 1958, doi: 10.1016/0022-3697(58)90033-7.

[165] H. Koizumi, S. Sharmin, K. Amemiya, M. Suzuki-Sakamaki, J.-I. Inoue, and H. Yanagihara, "Experimental evidence of orbital ferrimagnetism in $CoMnO_3$ (0001) epitaxial thin film," *Phys. Rev. Mater.*, vol. 3, no. 2, Feb. 2019, Art. no. 024404, doi: 10.1103/PhysRevMaterials.3.024404.

[166] H. Koizumi, J.-I. Inoue, and H. Yanagihara, "Magnetic anisotropy and orbital angular momentum in the orbital ferrimagnet $CoMnO_3$," *Phys. Rev. B, Condens. Matter*, vol. 100, no. 22, Dec. 2019, Art. no. 224425, doi: 10.1103/PhysRevB.100.224425.

[167] L. Šmejkal, J. Sinova, and T. Jungwirth, "Beyond conventional ferromagnetism and antiferromagnetism: A phase with nonrelativistic spin and crystal rotation symmetry," *Phys. Rev. X*, vol. 12, no. 3, Sep. 2022, Art. no. 031042, doi: 10.1103/PhysRevX.12.031042.

[168] L. Šmejkal, J. Sinova, and T. Jungwirth, "Emerging research landscape of altermagnetism," *Phys. Rev. X*, vol. 12, no. 4, Dec. 2022, Art. no. 040501, doi: 10.1103/PhysRevX.12.040501.

[169] L. Šmejkal, R. González-Hernández, T. Jungwirth, and J. Sinova, "Crystal time-reversal symmetry breaking and spontaneous Hall effect in collinear antiferromagnets," *Sci. Adv.*, vol. 6, no. 23, Jun. 2020, Art. no. aaz8809, doi: 10.1126/sciadv.aaz8809.

[170] D.-F. Shao, S.-H. Zhang, M. Li, C.-B. Eom, and E. Y. Tsymbal, "Spin-neutral currents for spintronics," *Nature Commun.*, vol. 12, no. 1, p. 3, Dec. 2021, doi: 10.1038/s41467-021-26915-3.

[171] R. González-Hernández, L. Šmejkal, K. Výborný, Y. Yahagi, J. Sinova, T. Jungwirth, and J. Železný, "Efficient electrical spin splitter based on nonrelativistic collinear antiferromagnetism," *Phys. Rev. Lett.*, vol. 126, no. 12, Mar. 2021, Art. no. 127701, doi: 10.1103/PhysRevLett.126.127701.

[172] S. Karube, T. Tanaka, D. Sugawara, N. Kadoguchi, M. Kohda, and J. Nitta, "Observation of spin-splitter torque in collinear antiferromagnetic RuO_2," *Phys. Rev. Lett.*, vol. 129, no. 13, Sep. 2022, Art. no. 137201, doi: 10.1103/PhysRevLett.129.137201.

[173] H. Bai, L. Han, X. Y. Feng, Y. J. Zhou, R. X. Su, Q. Wang, L. Y. Liao, W. X. Zhu, X. Z. Chen, F. Pan, X. L. Fan, and C. Song, "Observation of spin splitting torque in a collinear antiferromagnet RuO_2," *Phys. Rev. Lett.*, vol. 128, no. 19, May 2022, Art. no. 197202, doi: 10.1103/PhysRevLett.128.197202.

[174] I. I. Mazin, "Altermagnetism in MnTe: Origin, predicted manifestations, and routes to detwinning," *Phys. Rev. B, Condens. Matter*, vol. 107, no. 10, Mar. 2023, Art. no. L100418, doi: 10.1103/PhysRevB.107.L100418.

[175] R. D. Gonzalez Betancourt, J. Zubáč, R. Gonzalez-Hernandez, K. Geishendorf, Z. Šobáň, G. Springholz, K. Olejník, L. Šmejkal, J. Sinova, T. Jungwirth, S. T. B. Goennenwein, A. Thomas, H. Reichlová, J. Železný, and D. Kriegner, "Spontaneous anomalous Hall effect arising from an unconventional compensated magnetic phase in a semiconductor," *Phys. Rev. Lett.*, vol. 130, no. 3, Jan. 2023, Art. no. 036702, doi: 10.1103/PhysRevLett.130.036702.
[176] H. Reichlová, R. Lopes Seeger, R. González-Hernández, I. Kounta, R. Schlitz, D. Kriegner, P. Ritzinger, M. Lammel, M. Leiviskä, V. Petříek, P. Doležal, E. Schmoranzerová, A. Bad'ura, A. Thomas, V. Baltz, L. Michez, J. Sinova, S. T. B. Goennenwein, T. Jungwirth, and L. Šmejkal, "Macroscopic time reversal symmetry breaking by staggered spin-momentum interaction," 2020, *arXiv:2012.15651*.
[177] H. Yan, Z. Feng, P. Qin, X. Zhou, H. Guo, X. Wang, H. Chen, X. Zhang, H. Wu, C. Jiang, and Z. Liu, "Electric-field-controlled antiferromagnetic spintronic devices," *Adv. Mater.*, vol. 32, no. 12, Mar. 2020, Art. no. 1905603, doi: 10.1002/adma.201905603.
[178] Q. Shao, P. Li, L. Liu, H. Yang, S. Fukami, A. Razavi, H. Wu, K. Wang, F. Freimuth, Y. Mokrousov, M. D. Stiles, S. Emori, A. Hoffmann, J. Åkerman, K. Roy, J.-P. Wang, S.-H. Yang, K. Garello, and W. Zhang, "Roadmap of spin–orbit torques," *IEEE Trans. Magn.*, vol. 57, no. 7, pp. 1–39, Jul. 2021, doi: 10.1109/TMAG.2021.3078583.
[179] S. Y. Bodnar, L. Šmejkal, I. Turek, T. Jungwirth, O. Gomonay, J. Sinova, A. A. Sapozhnik, H.-J. Elmers, M. Kläui, and M. Jourdan, "Writing and reading antiferromagnetic Mn_2Au by Néel spin-orbit torques and large anisotropic magnetoresistance," *Nature Commun.*, vol. 9, no. 1, p. 348, Jan. 2018, doi: 10.1038/s41467-017-02780-x.
[180] Y. Saito, "Magnetic random access memory," in *Nanomagnetic Materials: Fabrication, Characterization and Applications*, A. Yamaguchi, A. Hirohata, and B. Stadler, Eds. Amsterdam, The Netherlands: Elsevier, 2021, pp. 50–486.
[181] T. Moriyama, W. Zhou, T. Seki, K. Takanashi, and T. Ono, "Spin-orbit-torque memory operation of synthetic antiferromagnets," *Phys. Rev. Lett.*, vol. 121, no. 16, Oct. 2018, Art. no. 167202, doi: 10.1103/PhysRevLett.121.167202.
[182] H. Masuda, T. Seki, Y.-C. Lau, T. Kubota, and K. Takanashi, "Interlayer exchange coupling and spin Hall effect through an Ir-doped Cu nonmagnetic layer," *Phys. Rev. B, Condens. Matter*, vol. 101, no. 22, Jun. 2020, Art. no. 224413, doi: 10.1103/PhysRevB.101.224413.
[183] H. Masuda, Y. Yamane, T. Seki, K. Raab, T. Dohi, R. Modak, K.-I. Uchida, J. Ieda, M. Kläui, and K. Takanashi, "Magnetization switching process by dual spin–orbit torque in interlayer exchange-coupled systems," *Appl. Phys. Lett.*, vol. 122, no. 16, p. 162402, Apr. 2023, doi: 10.1063/5.0140328.
[184] P. Qin, H. Yan, X. Wang, H. Chen, Z. Meng, J. Dong, M. Zhu, J. Cai, Z. Feng, X. Zhou, L. Liu, T. Zhang, Z. Zeng, J. Zhang, C. Jiang, and Z. Liu, "Room-temperature magnetoresistance in an all-antiferromagnetic tunnel junction," *Nature*, vol. 613, no. 7944, pp. 485–489, Jan. 2023, doi: 10.1038/s41586-022-05461-y.
[185] X. Chen, T. Higo, K. Tanaka, T. Nomoto, H. Tsai, H. Idzuchi, M. Shiga, S. Sakamoto, R. Ando, H. Kosaki, T. Matsuo, D. Nishio-Hamane, R. Arita, S. Miwa, and S. Nakatsuji, "Octupole-driven magnetoresistance in an antiferromagnetic tunnel junction," *Nature*, vol. 613, no. 7944, pp. 490–495, Jan. 2023, doi: 10.1038/s41586-022-05463-w.
[186] J. Dong, X. Li, G. Gurung, M. Zhu, P. Zhang, F. Zheng, E. Y. Tsymbal, and J. Zhang, "Tunneling magnetoresistance in non-collinear antiferromagnetic tunnel junctions," *Phys. Rev. Lett.*, vol. 128, no. 19, May 2022, Art. no. 197201, doi: 10.1103/PhysRevLett.128.197201.
[187] W. Zhou, T. Seki, T. Kubota, G. E. W. Bauer, and K. Takanashi, "Spin-Hall and anisotropic magnetoresistance in ferrimagnetic Co-Gd/Pt layers," *Phys. Rev. Mater.*, vol. 2, no. 9, Sep. 2018, Art. no. 094404, doi: 10.1103/PhysRevMaterials.2.094404.
[188] J. Wang, T. Seki, Y.-C. Lau, Y. K. Takahashi, and K. Takanashi, "Origin of magnetic anisotropy, role of induced magnetic moment, and all-optical magnetization switching for Co_{100-x} Gd_x/Pt multilayers," *APL Mater.*, vol. 9, no. 6, Jun. 2021, Art. no. 061110, doi: 10.1063/5.0050985.
[189] L. Šmejkal, J. Sinova, and T. Jungwirth, "Emerging research landscape of altermagnetism," 2022, *arXiv:2204.10844*.
[190] A. Hirohata and D. C. Lloyd, "Heusler alloys for metal spintronics," *MRS Bull.*, vol. 47, no. 6, pp. 593–599, Jun. 2022, doi: 10.1557/s43577-022-00350-1.

ATSUFUMI HIROHATA (Senior Member, IEEE) was born in Tokyo, Japan, in 1971. He received the B.Sc. and M.Sc. degrees in physics from Keio University, Japan, in 1995 and 1997, respectively, and the Ph.D. degree in physics from the University of Cambridge, U.K., in 2001.

From 2001 to 2002, he was a Postdoctoral Associate with The Cavendish Laboratory, University of Cambridge. In 2002, he moved to the Francis Bitter Magnet Laboratory, Massachusetts Institute of Technology, Cambridge, MA, USA, as a Postdoctoral Associate. He then became a Researcher with the Department of Materials, Tohoku University, Japan, in 2003, and the Frontier Research System, RIKEN, Japan, in 2005. He became a Lecturer with the Department of Electronics (now Department of Electronic Engineering), University of York, in 2007, and was promoted to a Reader, a Professor, and a Senior Professor, in 2011, 2014, and 2017, respectively. From 2015 to 2016, he was a Guest Professor (Global) with Keio University. From 2009 and 2017, he was a Visiting Professor with Tohoku University. Since October 2023, he is a Professor at the Center for Science and Innovation in Spintronics, Tohoku University, Japan. He edited three books and published more than 160 articles and 35 inventions. His research interests include spintronics and magnetic materials.

Prof. Hirohata is the President of the IEEE Magnetics Society and a member of the Administrative Committee of the Conference on Magnetism and Magnetic Materials. He was awarded an Industry Fellowship by the Royal Society, in 2013. He was a recipient of an Outstanding Presentation Award, in 2006, and a Young Scientist Award from The Magnetics Society of Japan, in 2005. He gave a Wohlfarth Memorial Lecture, in 2014. He is also a Deputy Editor of *Science and Technology of Advanced Materials*, an Editor of *Journal of Magnetism and Magnetic Materials*, *Spin* and *Magnetochemistry*, an Associate Editor of *Frontiers in Physics*, and an Editorial Board Member of *Journal of Physics D: Applied Physics*.

DAVID C. LLOYD was born in 1991. He received the M.Phys., M.Sc., and Ph.D. degrees in physics from the University of York, U.K., in 2013, 2015, and 2019, respectively.

From 2019 to 2020, he was with the Okinawa Institute of Science and Technology Graduate University, Japan, as a Postdoctoral Fellow. In 2021, he returned to the University of York as a Postdoctoral Research Associate. His research interests include in-situ electron microscopy, characterization of nanoscale materials, and the growth of functional magnetic materials.

TAKAHIDE KUBOTA (Member, IEEE) was born in Chiba, Japan, in 1982. He received the B.Eng., M.Eng., and Ph.D. degrees from Tohoku University, Japan, in 2005, 2007, and 2010, respectively. From 2010 to 2013, he was a Research Associate with the Advanced Institute for Materials Research, Tohoku University. In 2013, he moved to the Institute for Materials Research, Tohoku University, as an Assistant Professor. Since 2022, he has been a specially appointed Associate Professor with the Advanced Spintronics Medical Engineering, Graduate School of Engineering, Tohoku University. His research interests include spintronics and magnetic materials. He was awarded the 28th Tokin Science and Technology Award and the Special Award of Tokin Foundation by the Tokin Foundation for Advancement of Science and Technology, in 2018, and the 58th Harada Young Research Award by the Honda Memorial Foundation, Japan, in 2018.

TAKESHI SEKI was born in Shizuoka, Japan, in 1980. He received the B.Eng., M.Eng., and Ph.D. degrees from Tohoku University, Japan, in 2002, 2003, and 2006, respectively. From 2006 to 2008, he was a Postdoctoral Researcher with the Institute for Materials Research, Tohoku University. Then, he moved to the Graduate School of Engineering Science, Osaka University, Japan, as a Postdoctoral Researcher. In 2010, he became an Assistant Professor with the Institute for Materials Research, Tohoku University, and was promoted to an Associate Professor, in 2016. His research interests include the materials development for spintronics and nanomagnetism, the physics of spin transfer phenomena and spin current, and control of magnetization reversal and spin dynamics. He was awarded the Japan Institute of Metals and Materials 22nd Young Researcher Award, in 2012, The Magnetics Society of Japan Outstanding Research Award, in 2016, the 40th Honda Memorial Young Researcher Award, in 2019, and the Commendation for Science and Technology by the Minister of Education, Culture, Sports, Science and Technology, The Young Scientists' Prize, in 2019.

KOKI TAKANASHI (Senior Member, IEEE) was born in Tokyo, Japan, in 1958. He received the B.S., M.S., and Ph.D. degrees in physics from The University of Tokyo. From 1994 to 1995, he was an Alexander von Humboldt Research Fellow with Forschunszentrum Jülich, Germany. Then, he joined the Institute for Materials Research (IMR), Tohoku University, and was a Professor, from 2000 to 2022. He was the Director of IMR, from 2014 to 2020, and the Vice President with Tohoku University, from 2018 to 2020. He is currently the Director General of the Advanced Science Research Center, Japan Atomic Energy Agency. He was the leader of a national project in Japan ''Creation and Control of Spin Current,'' from 2007 to 2011. He has published more than 500 original and review papers. He has received numerous awards, including the Outstanding Research Award from The Magnetic Society of Japan (MSJ), in 2004, the Outstanding Paper Award from the Japan Society of Applied Physics (JSAP), in 2009, the Masumoto Hakaru Award from the Japan Institute of Metals and Materials (JIMM), in 2011, the Prize for Science and Technology of the Commendation from the Minister of Education, Culture, Sports, Science and Technology (MEXT), in 2018, the MSJ Society Award, in 2019, the JSAP Fellow Award, in 2019, and the Murakami Memorial Award, in 2021. He was also a Distinguished Lecturer of the IEEE Magnetic Society, in 2013, the President of MSJ, from 2017 to 2019, the President of the Asian Union of Magnetics Societies, from 2018 to 2019, and the President of JIMM, from 2020 to 2021.

HIROAKI SUKEGAWA (Member, IEEE) was born in Tokyo, Japan, in 1981. He received the M.Eng. and Ph.D. degrees in materials science from Tohoku University, Japan, in 2004 and 2007, respectively. He became a Researcher with the National Institute for Materials Science, in 2007, a Senior Researcher, in 2014, and a Principal Researcher, in 2018. He is currently the Group Leader of the Spintronics Group, Research Center for Magnetic and Spintronic Materials, National Institute for Materials Science. His research interests include magnetic thin films and spintronics devices. He was awarded the Outstanding Research Award by The Magnetics Society of Japan, in 2017, the Commendation for Science and Technology by the Minister of Education, Culture, Sports, Science and Technology, The Young Scientists' Prize, in 2020, and the AUMS Young Researcher Award by the Asian Union of Magnetic Societies, in 2020.

ZHENCHAO WEN was born in Hebei, China, in 1981. He received the B.S. degree in physics from Lanzhou University, China, in 2005, and M.S. and Ph.D. degrees in condensed matter physics from the Institute of Physics, Chinese Academy of Sciences, in 2007 and 2010, respectively. From 2010 to 2015, he was a Postdoctoral Researcher with the National Institute for Materials Science (NIMS), Japan, where he has been a Senior Researcher, since 2018. In 2015, he moved to the Institute for Materials Research, Tohoku University, as a Postdoctoral Researcher, and a specially appointed Assistant Professor, in 2016. His research interests include spintronics and magnetic materials, especially, magnetic tunnel junctions, Heusler alloys, and topological materials.

SEIJI MITANI was born in Kochi, Japan, in 1965. He received the M.Eng. and Ph.D. degrees in materials science from Nagoya University, Japan, in 1990 and 1993, respectively.

In 1993, he became a Research Associate with the Institute for Materials Research and was promoted to an Associate Professor, in 2001. In 2008, he moved to the Magnetic Materials Unit, National Institute for Materials Science (NIMS), as a Researcher, and became the Group Leader of the Spintronics Group. Since 2010, he has been an Adjunct Professor with the Graduate School of Pure and Applied Sciences, University of Tsukuba. Since 2021, he has also been the Director of the Research Center for Magnetic and Spintronic Materials, NIMS. His research interests include spintronics and magnetic materials.

Dr. Mitani was a recipient of the Japan Institute of Metals and Materials Young Researcher Award, in 1997, and the Outstanding Presentation Award from The Magnetic Society of Japan (MSJ), in 2005.

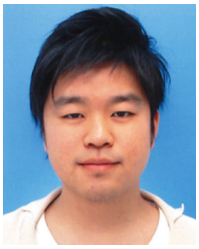

HIROKI KOIZUMI was born in Ibaraki, Japan, in 1994. He received the B.S. degree in physics from the Tokyo Institute of Technology, Japan, in 2017, and the M.Eng. and Ph.D. degrees in applied physics from the University of Tsukuba, Japan, in 2019 and 2022, respectively. From 2022 to 2023, he was a Postdoctoral Researcher with the National Institute for Materials Science (NIMS), Japan. In 2023, he moved to the Center for Science and Innovation in Spintronics (CSIS), Tohoku University, as an Assistant Professor. His research interests include spintronics and magnetic materials.